CCC Annual Report

UIUC, August 14, 2013

Modeling and Simulation of Multiphase Flows in CC Mold Region

Rui Liu

Department of Mechanical Science & Engineering
University of Illinois at Urbana-Champaign

Outline

- **Determination of slide-gate position (PART 1)**
  - Using a gate-position-based flow rate model to back-calculate gate position based on measured casting speed and mold dimensions;
- **Gas flow through UTN and bubble size (PART 2)**
  - To predict hot argon flow rate entering steel stream;
  - To estimate active sites number density at UTN inner surface
  - To predict initial bubble size
- **Multi-phase flow modeling (PART 3)**
  - Board 4
  - Board 11~13
  - Board 14~16

and Validation with nailboard measurements:
  - Surface velocity profile
  - Surface level profile

also, Parametric study on bubble size effects

Acknowlegements

- Continuous Casting Consortium Members
(ABB, ArcelorMittal, Baosteel, Magnesita Refractories, Nippon Steel, Nucor Steel, Postech/ Posco, Severstal, SSAB, Tata Steel, ANSYS/ Fluent)
- **J. Powers and T. Henry in Severstal for the help with the plant nail board trials on Oct. 15~16 in Severstal in Dearborn, MI, the caster of which has:**
  - a 203 mm mold thickness
  - plant operation data recorded for gate position, flow rate, mold level, casting speed, …
- **R. Singh for the help with nail board experiments**
- **Mihir Chavan for the nail board measurements**

PART 1:
Gate Position Estimation

Modeling SEN Flow Rate

--Analysis of Bernoulli's Equation

$$\frac{p_0}{\rho g}+\cancelto{0}{\frac{v_0^2}{2g}}+z_0=\frac{p_3}{\rho g}+\frac{v_3^2}{2g}+z_3+h_{port}+h_f+h_{sg}$$

$$p_0 = 1.01\times 10^5\,Pa$$

$$p_3=\rho g H_3+p_0$$

$$z_0-z_3=H_1+H_2+H_3$$

$$\underbrace{\frac{p_0-p_3}{\rho g}}_{-H_3}+\underbrace{z_0-z_3}_{H_1+H_2+H_3}=\frac{v_3^2}{2g}+\sum h \rightarrow h_{port}+h_f+h_{sg}$$

$$h_{port}=\frac{v_{SEN}^2}{2g}\left(\frac{A_{SEN}}{A_{port}}-1\right)^2 \qquad h_f=f\frac{L_{SEN}}{D_{SEN}}\frac{v_{SEN}^2}{2g}$$

$$\boxed{h_{sg}=\left(\left(\frac{1}{\mu}-1\right)^2\left(\frac{A_{SEN}}{A_{GAP}}\right)^2+\left(\frac{A_{SG}}{A_{GAP}}-\frac{A_{GAP}}{A_{SG}}\right)^2\left(\frac{A_{SEN}}{A_{SG}}\right)^2\right)\frac{v_{SEN}^2}{2g}}$$

$$\mu=\frac{A_{vc}}{A_{SG}}=\begin{cases}0.63+0.37\left(\dfrac{A_{GAP}}{A_{SG}}\right)^3 & \textbf{correlation 1[1]}\\ 0.5864+0.2762\left(\dfrac{A_{GAP}}{A_{SG}}\right)-0.4807\left(\dfrac{A_{GAP}}{A_{SG}}\right)^2+0.618\left(\dfrac{A_{GAP}}{A_{SG}}\right)^3 & \textbf{cor. 2[2]}\\ 0.64 & \textbf{cor. 3[3]}\end{cases}$$

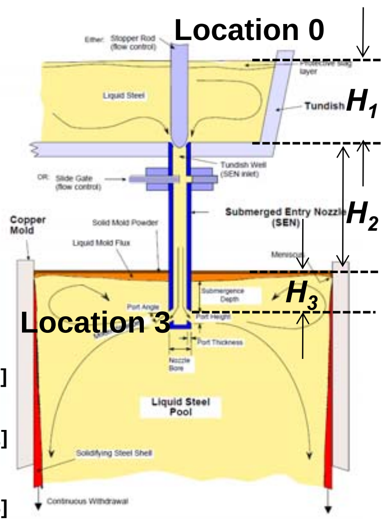

Ref:

[1] Oertel, Herbert; Prandtl, Ludwig, et.al, Prandtl's Essentials of Fluid Mechanics, Springer, ISBN 0387404376. See pp. 163–165.

[2] Evangelista Torricelli, 1643; [3] http://en.wikipedia.org/wiki/Vena_contracta

Gate-position-based Model (considering gas addition)

- **Equation for gate-position-based model [1]:**

$$Q_{SEN}=A_{eff}\sqrt{\frac{2g\left(H_1+H_2\right)}{\left(\frac{A_{SEN}}{A_{port}}-1\right)^2+f\frac{L_{SEN}}{D_{SEN}}+\left(\frac{1}{\mu}-1\right)^2\left(\frac{A_{SEN}}{A_{GAP}}\right)^2+\left(\frac{A_{SG}}{A_{GAP}}-\frac{A_{GAP}}{A_{SG}}\right)^2\left(\frac{A_{SEN}}{A_{SG}}\right)^2+\left(\frac{A_{SEN}}{2A_{port}}\right)^2}}$$

where $\mu=0.63+0.37\left(\dfrac{A_{GAP}}{A_{SG}}\right)^3$ $\quad A_{eff}=\begin{cases}A_{SEN} & \textbf{single phase flow}\\ \dfrac{V_cWT}{Q_{gas}+V_cWT}A_{SEN} & \textbf{two phase flow}\end{cases}$

For continuous caster, an extra term should be added to account for pressure drop due to clogging:

$$Q_{SEN}=A_{eff}\sqrt{\frac{2g\left(H_1+H_2\right)}{\left(\frac{A_{SEN}}{A_{port}}-1\right)^2+f\frac{L_{SEN}}{D_{SEN}}+\left(\frac{1}{\mu}-1\right)^2\left(\frac{A_{SEN}}{A_{GAP}}\right)^2+\left(\frac{A_{SG}}{A_{GAP}}-\frac{A_{GAP}}{A_{SG}}\right)^2\left(\frac{A_{SEN}}{A_{SG}}\right)^2+\left(\frac{A_{SEN}}{2A_{port}}\right)^2+C}}$$

In current study, *C=0* is assumed (no clogging).

Validation for Gate-position-based Model

--using full-scale water model measurements at ArcelorMittal, East Chicago

- **Nice match is observed, analytical SEN flow rate model is validated**
- **Gap area is [1]:**

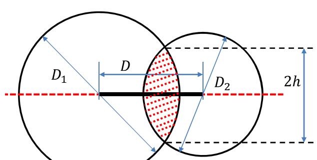

$$h = \frac{D_1 D_2}{4D}\sqrt{1-\left(\frac{D_1^2+D_2^2-4D^2}{2D_1 D_2}\right)^2}$$

$$A_{GAP} = \frac{D_1^2}{4}\arcsin\left(\frac{2h}{D_1}\right)+\frac{D_2^2}{4}\arcsin\left(\frac{2h}{D_2}\right)-Dh, \quad if \quad D > \frac{\sqrt{D_1^2-D_2^2}}{2}$$

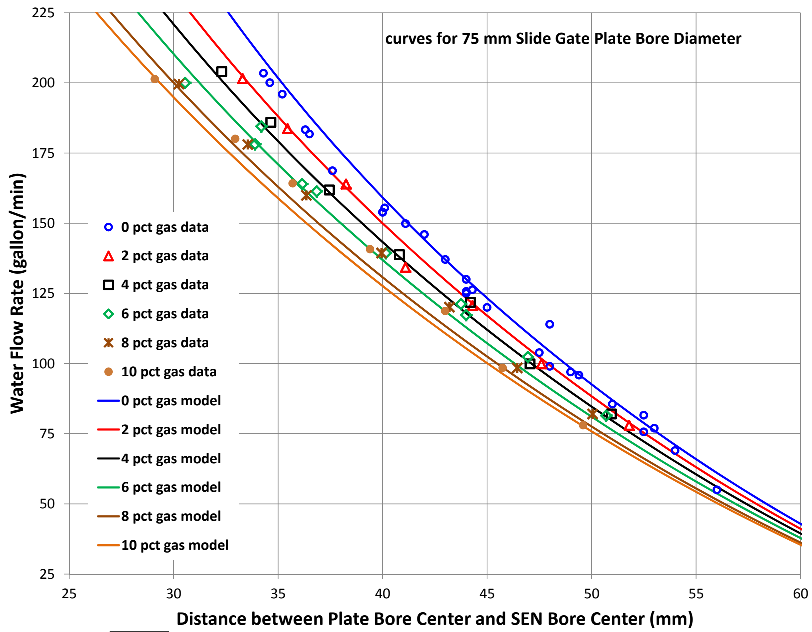

R. Liu, B.G. Thomas, B. Forman and H. Yin,, AISTech Iron Steel Technol. Conf. Proc., 2012, Atlanta, GA, pp 1317.

Predicted vs. Measured Gate Position at Severstal

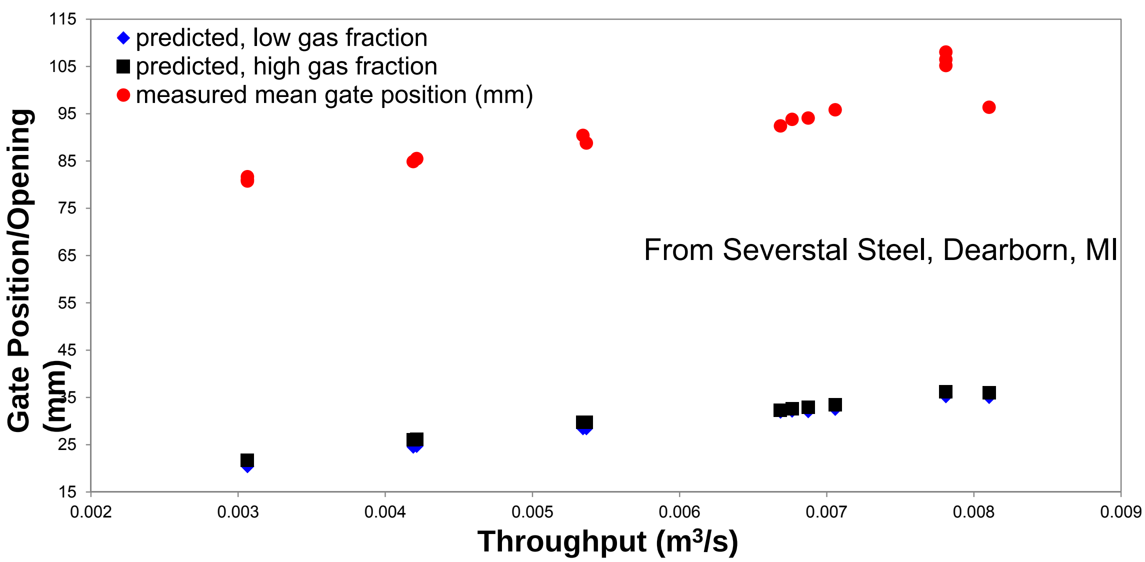

Low/High gas fraction indicates the location where the fraction is calculated:
Low fraction is calculated at UTN gas injection point;
High fraction is calculated at SEN port exit.

Predicted vs. Calibrated Measurements

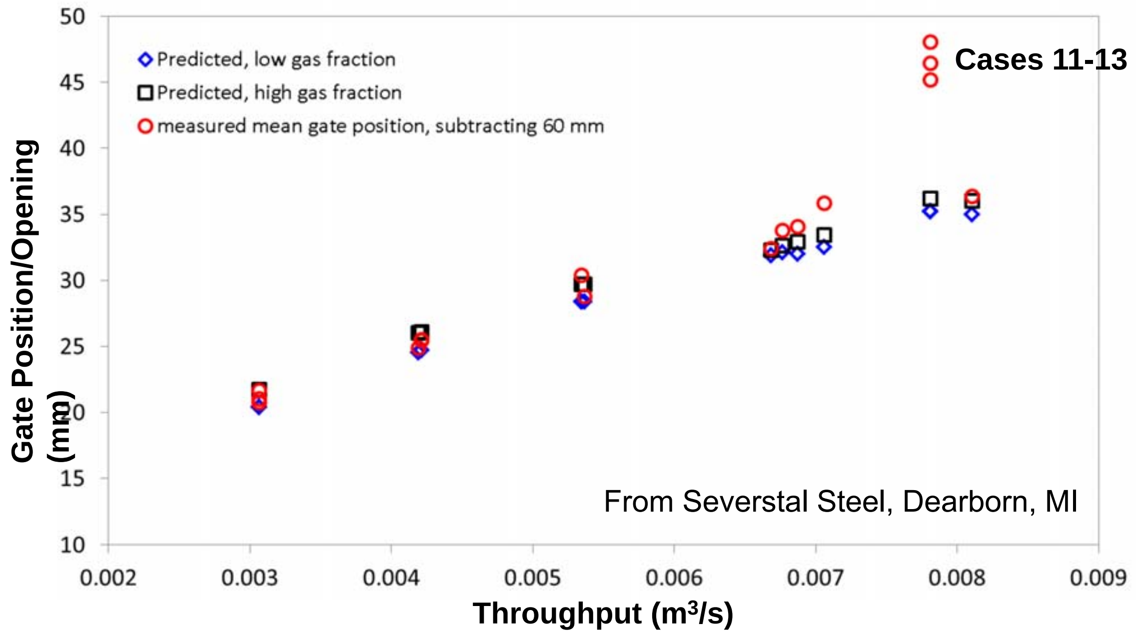

Exact offset for quantitative gate position not recorded, but typically is 40-60mm

Part 1. Gate-position Conclusions

- **Prediction and measurements show the same trend at different throughputs;**
- **Once the measured gate position is calibrated by subtracting 60 mm, the predicted gate position usually matches closely with measurements; mismatch is restricted to one set of casting conditions (case 11~13);**
- **Gas flow (< 8%) has little effect on gate position (for range of conditions studied)**

Continuous Casting Consortium

PART 2:
UTN Gas Flow Simulation and Initial Bubble Size Distribution

Continuous Casting Consortium

Methodology of Initial Bubble Size Estimation in Argon-Steel System

Calculate the Gas Velocity profile at UTN/SEN inner surface ← via solving a Porous-Flow /Pressure-Source model for average normal velocity at UTN inner surface (described previously) [1]

↓

Active Sites Number Density Distribution at UTN inner surface ← via empirical equation from G. Lee and B.G. Thomas [2]

for gas injection at UTN or SEN refractory

↓

Calculation of Gas Volume Flux per Active Site ← (Total Flow Rate/cm^2)/(Active sites #/cm^2)

↓

Estimation of Mean Diameter of Initial Bubble Formation ← via two-stage model from H. Bai and B.G. Thomas [3]

References:
[1]
R. Liu and B.G. Thomas, Iron and Steel Technology Conference Proceedings, p 2235-2245, 2012, AISTech

[2]
G. Lee, B.G. Thomas, et al., Met. Mater. Int., Vol. 16, No. 3 (2010), pp. 501~5063

[3]
H. Bai and B.G. Thomas, Metall. Mater. Trans. B 32,

Governing Equations
-- Pressure-Source Model

Darcy's Law: $\mathbf{v} = -K_D \nabla p$ **(1)**

Mass Conservation (or continuity): $\nabla \cdot (\rho \mathbf{v}) = 0$ **(2)**

Heat Conduction: $\nabla \cdot (k \nabla T) = 0$ **(3)**

Ideal Gas Law: $p = \rho R T$ **(4)**

Eqn (1) and (2) $\Rightarrow$ $\nabla \cdot (\rho K_D \nabla p) = 0$ $\Rightarrow$ $\nabla \rho \cdot (K_D \nabla p) + \rho \nabla \cdot (K_D \nabla p) = 0$

$$\Rightarrow \left.\begin{aligned} \nabla \cdot (K_D \nabla p) &= -\frac{1}{\rho}\left[\nabla \rho \cdot (K_D \nabla p)\right] \\ \rho &= \frac{p}{RT} \end{aligned}\right\} \Rightarrow \boxed{\nabla \cdot (K_D \nabla p) = -\frac{RT}{p}\left[\nabla\left(\frac{p}{RT}\right)\cdot (K_D \nabla p)\right] = \dot{S}}$$

pressure diffusion

Pressure source due to gas expansion

-- **For Pressure-Source Model**

- The **left hand side** of the final equation above (in red box) is the standard diffusion part, while the **right hand side is in the form of a source term taking into account the effect of gas expansion due to temperature and pressure gradient**.
- Using a 3-D FLUENT model, adding a source term to pressure (or a user-defined-scalar) diffusion equation coupling the energy equation

Governing Equations
-- Porous Flow Model

Mass Conservation (or continuity): $\nabla \cdot (\rho \mathbf{v}) = 0$ **(1)**

Heat Conduction: $\nabla \cdot (k \nabla T) = 0$ **(2)**

Ideal Gas Law: $p = \rho R T$ **(3)**

Full Set of Navier-Stokes Equations for flow in porous media:

$$\nabla \cdot (\rho \mathbf{v}\mathbf{v}) \sim \frac{\rho V^2}{\Delta r} = \frac{0.3 \times 0.0073^2}{0.035} \approx 4.6 \times 10^{-4}$$

viscous resistance

Re ~2.3, C=0 for laminar flow

$$\cancel{\frac{\partial(\rho \mathbf{v})}{\partial t}} + \cancel{\nabla \cdot (\rho \mathbf{v}\mathbf{v})} = -\nabla p + \cancel{\nabla \cdot (\mu \nabla \mathbf{v})} + \mathbf{F} - \left(\frac{\mu}{\alpha}\mathbf{v} + \cancel{C\frac{1}{2}\rho|\mathbf{v}|\mathbf{v}}\right) \qquad \frac{\mu}{\alpha} = \frac{1}{K_D}$$

0 (steady state problem)

0

0

0

$$\nabla \cdot (\mu \nabla \mathbf{v}) \sim \frac{\mu V}{\Delta r^2} = \frac{8.1 \times 10^{-5} \times 0.0073}{0.035^2} = 4.8 \times 10^{-4}$$

inertial resistance

$$\Rightarrow \mathbf{v} = -K_D \nabla p$$

-- **Porous-Flow Model**

- Solve a complete set of Navier-Stokes equations, with the momentum equation simplified into equation (1), adopting the ideal gas law to relate density with pressure and temperature.

Permeability Formulation

- **About permeability in Darcy's law:**
  - **Permeability measured the viscous resistance of the porous media to fluid;**
  - **Actual permeability consists of specific permeability and gas dynamic viscosity: specific permeability keeps constant for a chosen refractory and argon dynamic viscosity changes with local temperature.**

Permeability Varying with Temperatrue:

$$K_D = \frac{K_{DS}}{\mu(T)} \quad \begin{cases} K_{DS} = 1.01\times10^{-12} m^2 & \text{(constant specific permeability, from draft paper)} \\ \mu(T) & \text{(gas dynamic viscosity, as a function of local temperature)} \end{cases}$$

Viscosity Varying with Temperatrue: $\log\,[\eta(T)/\eta(293)] = 0.63842\,\log\,T - 6.9365/T - 3374.72/T^2 - 1.51196$ **Ref[1]**

or $\mu(T) = \mu_0 * 10^{\left(0.63842\lg T - 6.9365/T - 3374.72/T^2 - 1.51196\right)}$ $\quad \mu_0 = 2.228\times10^{-5}\,Pa\cdot s$

Room temperature (20 C) argon viscosity

Ref:
[1] R. Dawe and E. Smith. Viscosity of Argon at High Temperatures. Science, Vol. 163, pp 675~676, 1969.

Domain, Mesh and Temperature for Porous Gas Flow Model in Severstal UTN

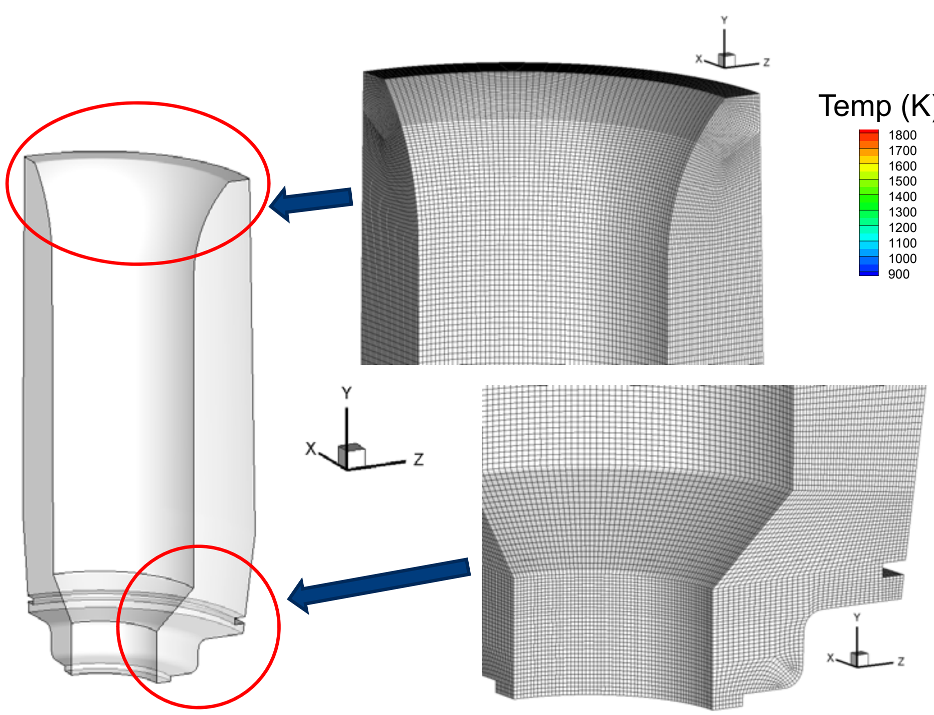

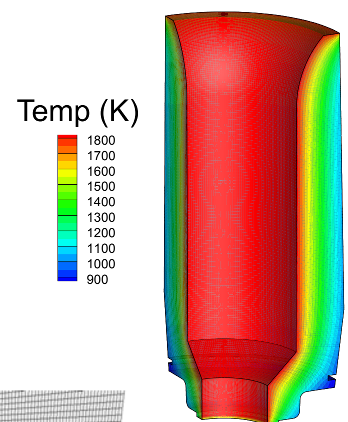

Total 0.6 million mapped hexahedral cells for quarter domain

Parameters

Specific Permeability (npm)	Back Pressure (Psi)	Measured Argon Flow Rate (SLPM)
10.1	15.45	5.02

Boundary Conditions:

Parameters	Values
h_{inner} (W/m^2K)	**$2.5*10^4$**
h_{outer} (W/m^2K)	**10**
Heat conductivity K_s (W/mK)	**33**
μ (Pa*s)	**0.0056**
ρ (kg/m^3)	**7200**
Average steel velocity U (m/s)	**1.6**

Symmetric B.C.

Pressure B.C. at UTN inner surface (with/without pressure correction using Bernoulli's equation)

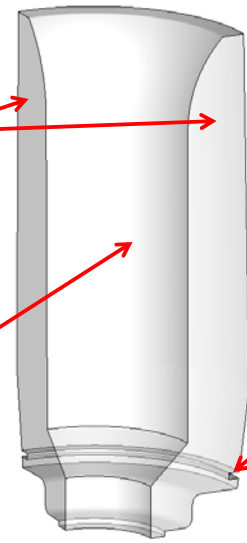

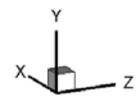

Wall B.C. at anywhere else

Pressure B.C. at gas slot

Pressure Distribution

With/Without using Bernoulli's Equation for Inner Surface Pressure Estimation

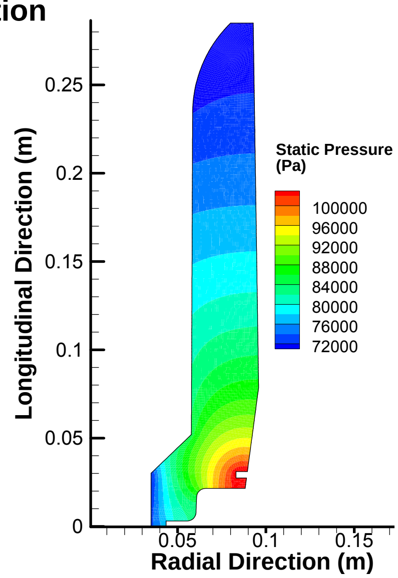

With Bernoulli's Equation for Inner Surface Pressure including hydrostatic &velocity terms

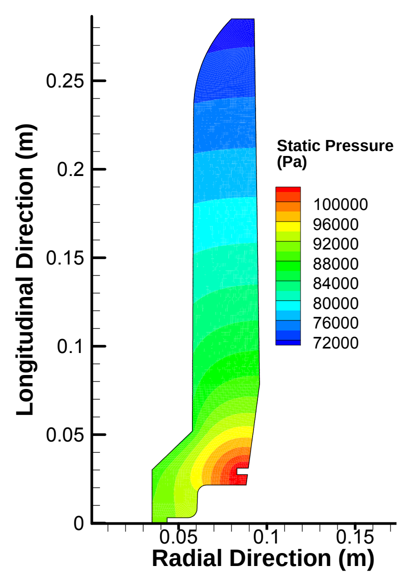

Hydrostatic Pressure only on Inner Surface

Gas Velocity Distribution

With/Without steel velocity effect on inner surface pressure

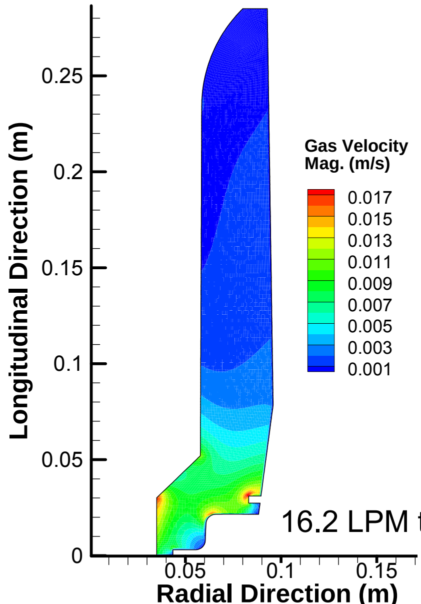

using Bernoulli's Equation for Inner Surface Pressure Estimation

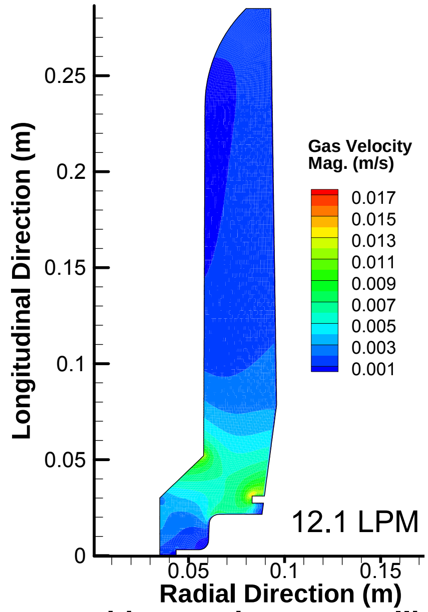

Without using Bernoulli's Equation

Gas Velocity Distribution (3-D View)

using Bernoulli's Equation for Inner Surface Pressure Estimation

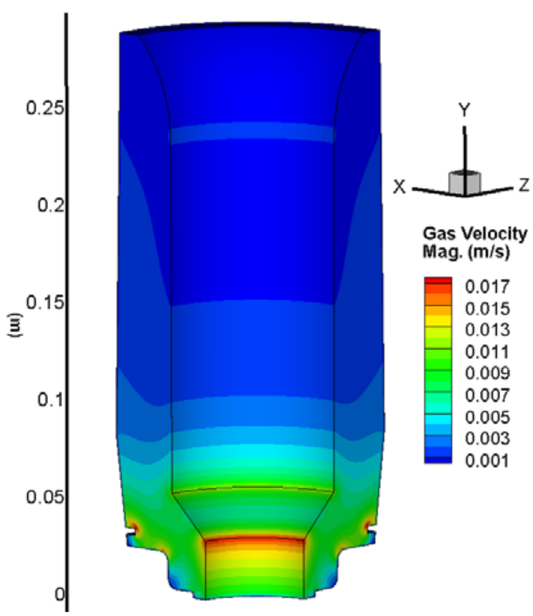

Without using Bernoulli's Equation

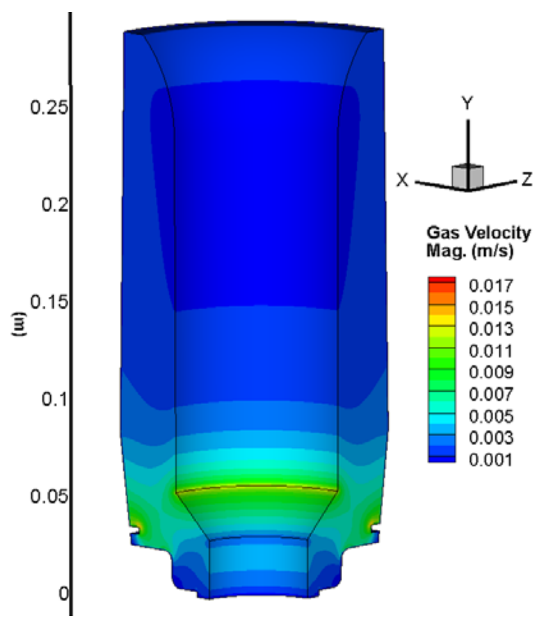

Gas Flow Simulation

- **Velocity Distribution (with/without pressure correction using Bernoulli's equation)**

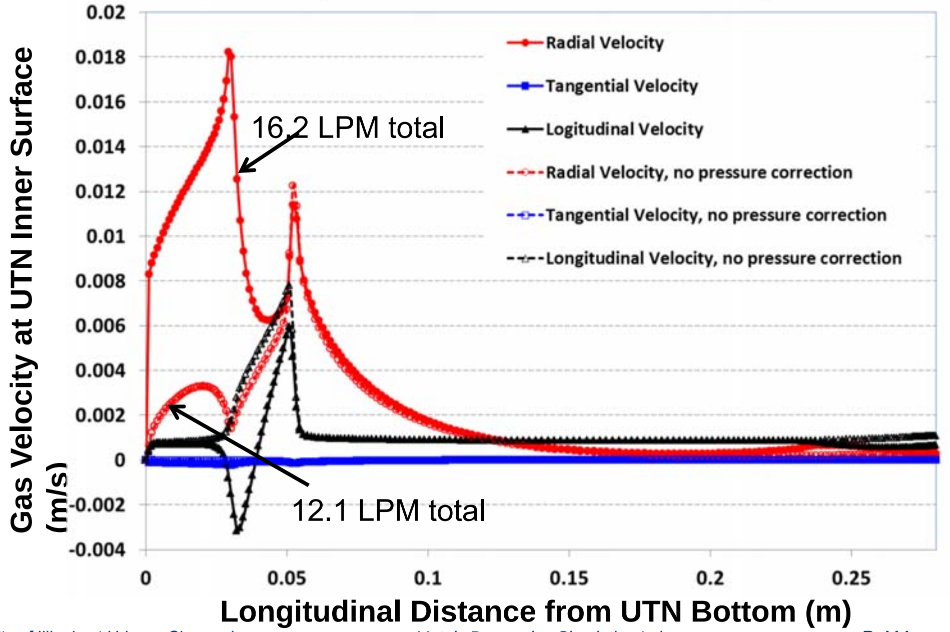

Calculating Gas Flow Rate

$$pV = nRT$$

$$\frac{pV}{T} = nR$$

$$\frac{p_{hot}V_{hot}}{T_{hot}} = nR = \frac{p_{std}V_{std}}{T_{std}}$$

$$\frac{p_{hot}Q_{hot}\Delta t}{T_{hot}} = \frac{p_{std}Q_{std}\Delta t}{T_{std}}$$

$$\int_S \frac{p_{hot}Q_{hot}\Delta t}{T_{hot}} dS = \int_S \frac{p_{std}Q_{std}\Delta t}{T_{std}} dS$$

$$SQ_{std} = \frac{T_{std}}{p_{std}T_{hot}} \int_S p_{hot}Q_{hot} dS$$

T_{std} (K)	T_{hot} (K)	P_{std} (Pa)	K_d (npm)
300	1832	101325	10.1

p_{hot} and Q_{hot} are the absolute pressure and gas hot flow rate at each of the face centers from the simulated data, then integrate them over the UTN inner surface to evaluate the gas volume flow rate in standard conditions as shown in the equation.

Since only a quarter is modeled, the total flow rate will be 4 times of the calculated value of $S*Q_{std}$.

$$\dot{V}_{total,std} = 4SQ_{std} = 4*1.9156\times10^{-5} = 7.6624\times10^{-5}\ m^3/s$$

In SLPM, it is: 7.6624*10^{-5}*1000*60 = 4.6 SLPM, which matches reasonably well with measured gas flow rate of 5.01 SLPM. The mismatch could be caused by using a different permeability in the simulation, or possible gas leakage.

Estimation of Active Sites Number at UTN Refractory Inner Surface

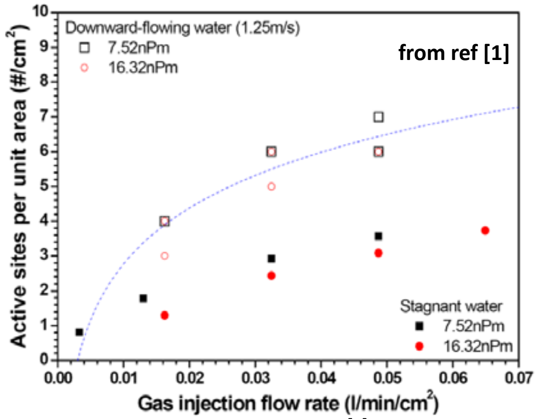

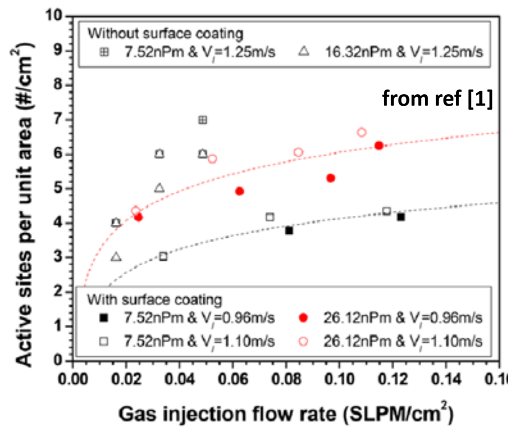

G. Lee and B.G. Thomas suggest[1]:

$$\text{Active sites per unit area}\,(\#/\text{cm}^2) = 7 \times \frac{Q_g^{0.2635} \times U^{0.85} \times P_{erm}^{0.3308}}{Radians(\theta)}$$

Where:

- Q_g: the gas injection flow rate per cm^2 (LPM);
- U: liquid superficial velocity (m/s);
- P_{erm}: material permeability (npm);
- ϑ: contact angle for wettability (rad)

So the number of active sites per cm^2 is:

$$N_{site} = \frac{7Q_g^{0.2635}U^{0.85}P_{erm}^{0.3308}}{\theta}$$

Ref:
[1] G. Lee, B.G. Thomas, et al., Met. Mater. Int., Vol. 16, No. 3 (2010), pp. 501~506

Estimation of Mean Bubble Size using a Two-Stage Model

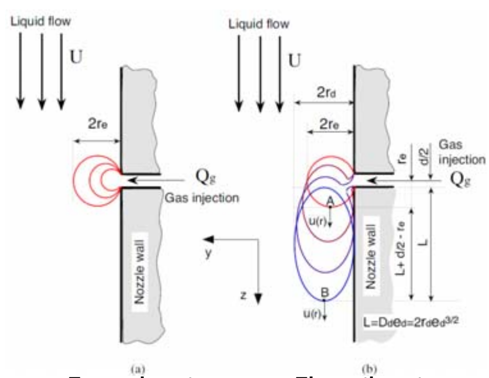

Expansion stage Elongation stage

--Figures from ref [2]

Active sites function as drilled holes where gas is injected. So based on the number of active sites and gas flow rate over an area, the gas flow rate per active site can be determined.

Ref:
[2] H. Bai and B. G. Thomas, Metall. Mater. Trans. B 32, 1143(2001).

Hua Bai's two-stage initial bubble formation model[2]:

1. **Expansion stage (solving for r, as r_e)**

$$\boxed{C_D \frac{1}{2}\rho_l \bar{u}^2 \pi r^2 = \frac{4}{3}\pi r^3(\rho_l - \rho_g)g + \frac{1}{2}\pi r \sigma \sin\theta_O(\cos\theta_r - \cos\theta_a)}$$

Drag coefficient: $C_D = \frac{24}{\mathrm{Re}_{bub}}(1+0.15\mathrm{Re}_{bub}^{0.687}) + 0.42/(1+4.25\times10^4\,\mathrm{Re}_{bub}^{-1.16})$

Bubble Reynolds number: $Re_{bub} = \frac{\bar{u}D}{\upsilon}$

$$\bar{u} = \frac{1}{2r}\int_{y=0}^{y=2r} u\,dy = 1.3173U\frac{r^{1/7}}{D_N^{1/7}}$$

Based on the 1/7th law in turbulent flow in the circular pipe

Contact angle function: $f_\theta = \sin\theta_o(\cos\theta_r - \cos\theta_a)$

$$f\theta(U) = -0.06079 + 0.33109U(m/s) + 0.078773U(m/s)^2$$

Empirical correlation with liquid steel superficial velocity

2. **Elongation stage (solving for r_d)**

$$\boxed{5.2692\frac{\pi U}{Q_g D_N^{1/7}}\int_{r_e}^{r_d}\left(r^{15/7}(ar+b)^{3/2} + \frac{ar^{22/7}}{2}(ar+b)^{1/2}\right)dr = 2r_d e_d^{3/2} + \frac{d}{2} - r_e}$$

$$a = \frac{e_d - 1}{r_d - r_e} \quad b = \frac{r_d - e_d r_e}{r_d - r_e} \quad e_d = 0.78592 + 0.70797U(m/s) - 0.12793U(m/s)^2$$

- D_N :nozzle inner diameter (m)
- ρ_l :liquid density (kg/m^3)
- ρ_g :gas density (kg/m^3)
- U :liquid steel superficial velocity (m/s)
- σ :surface tension (N/m)
- υ :kinematic viscosity of liquid steel (Pa*s)

Initial Bubble Size Distribution at UTN Inner Surface

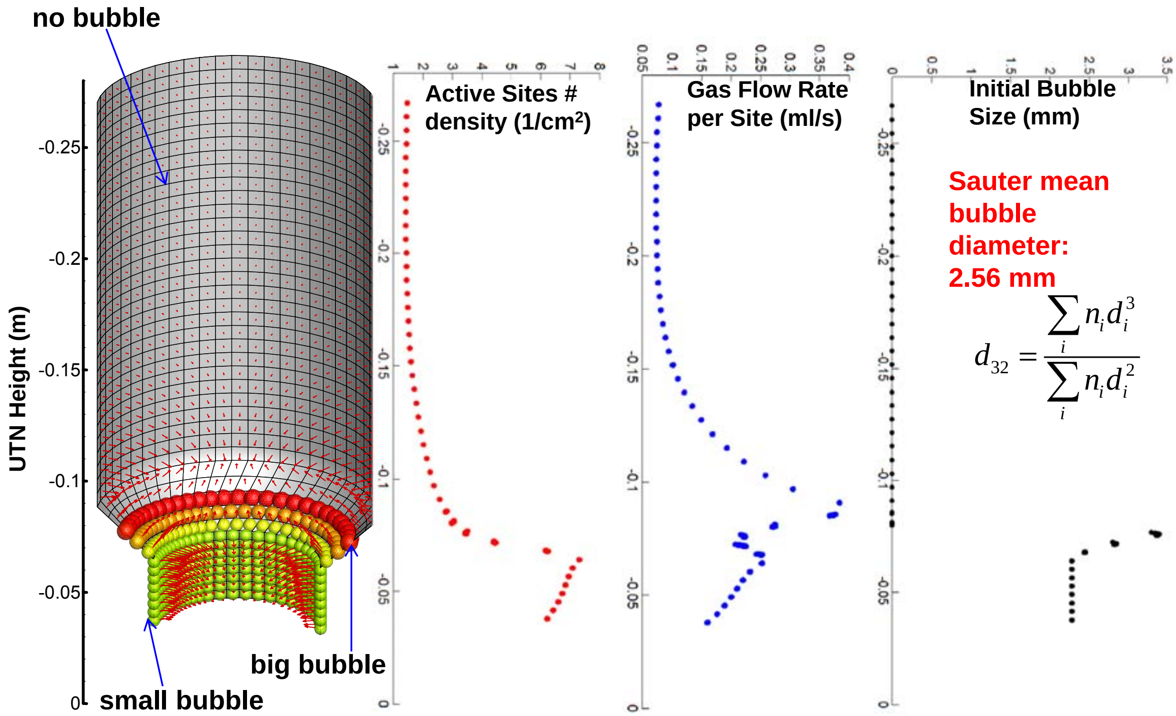

$$d_{32} = \frac{\sum_i n_i d_i^3}{\sum_i n_i d_i^2}$$

PART 2 Conclusion

- Pressure at UTN inner surface serves as a boundary condition in the simulation of heated gas flow through porous refractory, thus needs careful treatment. Two different treatments of inner surface pressure were applied in current study:
  - Hydrostatic pressure only;
  - Hydrostatic pressure with correction using Bernoulli’s equation (considering fluid kinetic energy change and pressure loss due to flow area change inside UTN)
- Results show:
  - Without pressure correction, hot argon flow rate is 12.1 LPM;
  - With pressure correction, hot argon flow rate is 16.2 LPM

PART 2 Conclusion

- A model system has been established to calculate hot argon flow rate at UTN inner surface, and estimate the active sites number density and eventually initial bubble size distributions.
- The initial bubble size is then used as an input parameter for multiphase flow simulations.
- For Severstal conditions for Nail Board 4,
  – Active sites number density ranges from 0 to ~7 /cm^2;
  – Initial bubble size ranges from ~2.2 to ~3.5 mm, with a Sauter-mean diameter = 2.56 mm;
  – Corresponding bubbling frequency ranges from ~40 to ~180 Hz.

PART 3:

Multi-phase Flow Simulations with Nail-Board Measurements

Model Assumptions and Computational Details

- **Model assumptions:**
  - **Isothermal flow**
  - **Argon-steel flow is within bubbly flow regime**
  - **No argon bubble break-up or coalescence, bubble size doesn't change with local pressure**
  - **Left-right symmetry for nozzle and mold domains**
  - **Relatively calm top surface, no significant gravity waves exist**

Governing Equations for Single-Phase Flow in Nozzle/Mold Region

- **Continuity Equation:** $\nabla\cdot(\rho\mathbf{v})=0$
- **Momentum Conservation – Navier-Stoke Equation:**

$$\frac{\partial(\rho\mathbf{v})}{\partial t}+\nabla\cdot(\rho\mathbf{v}\mathbf{v})=-\nabla p+\nabla\cdot\left(\left(\mu+\mu_T\right)\nabla\mathbf{v}\right)+\rho\mathbf{g}$$

- **Turbulence Model – *k-ω* SST URANS model [1]:**

k **equation:**

$$\frac{\partial k}{\partial t}+\mathbf{v}\cdot\nabla k=P_k-\beta^* k\omega+\nabla\cdot\left(\left(\nu+\sigma_k\nu_T\right)\nabla k\right)$$

Omega **equation:**

$$\frac{\partial\omega}{\partial t}+\mathbf{v}\cdot\nabla\omega=\alpha S^2-\beta\omega^2+\nabla\cdot\left(\left(\nu+\sigma_\omega\nu_T\right)\nabla\omega\right)+2\left(1-F_1\right)\sigma_{\omega 2}\frac{1}{\omega}\left(\nabla k\cdot\nabla\omega\right)$$

$$\nu_T=\frac{a_1 k}{\max\left(a_1\omega, SF_2\right)}=\frac{\mu_T}{\rho}$$

Values for the closure parameters can be found in [1].

[1] F.R. Menter, "Two-Equation Eddy-Viscosity Turbulence Models for Engineering Applications", *AIAA Journal*, 1994, **32**(8), pp 1598

Domain, Mesh and Methods for Fluid Flow in Severstal Caster Nozzle and Mold

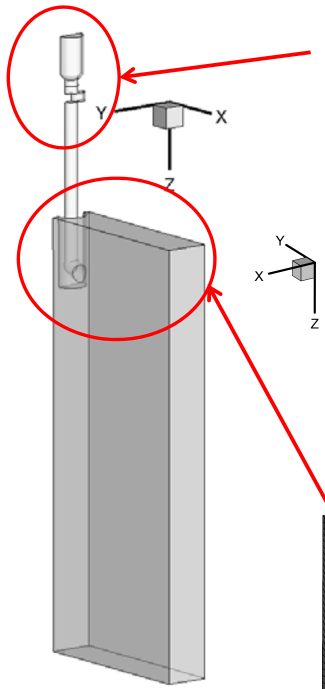

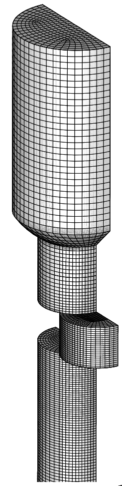

Models and Schemes	Name
Turbulence Model	*k-ω* model
Multiphase Model	Eulerian Model
Advection Discretization	2^{nd} order upwinding scheme

B.C.:

Meniscus	Domain Outlet
Free-slip wall with Gas Sink	Pressure outlet

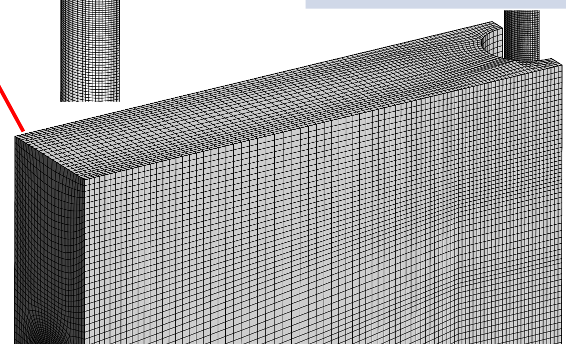

Time step:
0.05 sec

Total mesh:
0.45 million mapped hexa- cells

BOARD 4: Single Phase Flow Pattern Evolution -- note jet wobble (~20s period)

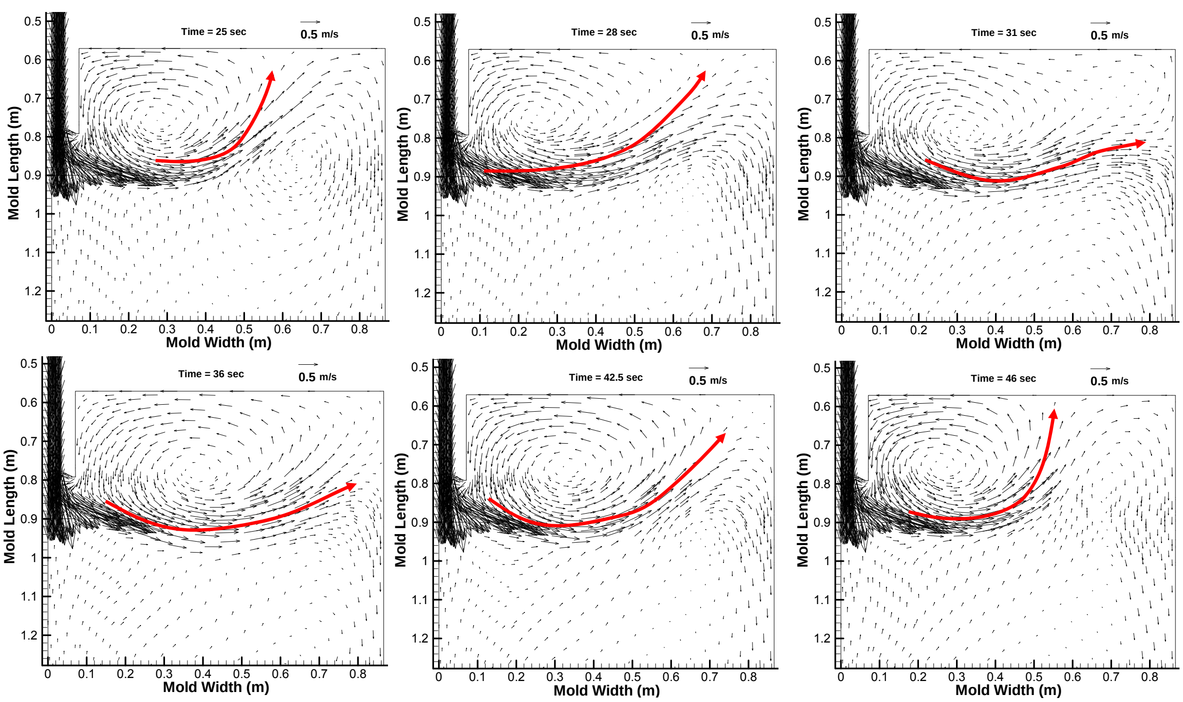

Single Phase Liquid Steel Flow Pattern -- Movie

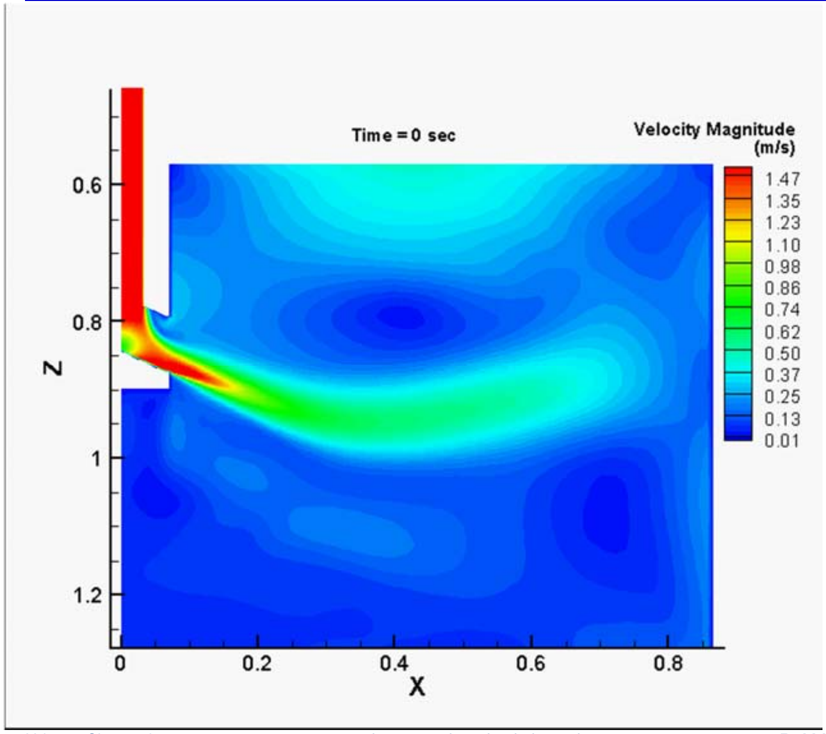

Multiphase Flow Models – Eulerian Bubble Model

- **Eulerian-Eulerian Model, treat argon gas as another continuous phase**

Continuity for argon: $$\frac{\partial(\alpha_a \rho_a)}{\partial t} + \nabla \cdot (\alpha_a \rho_a \mathbf{v}_a) = 0$$

Continuity for steel: $$\frac{\partial(\alpha_s \rho_s)}{\partial t} + \nabla \cdot (\alpha_s \rho_s \mathbf{v}_s) = 0$$

Momentum balance for argon:

$$\frac{\partial(\alpha_a \rho_a \mathbf{v}_a)}{\partial t} + \nabla \cdot (\alpha_a \rho_a \mathbf{v}_a \mathbf{v}_a) = -\alpha_a \nabla p + \nabla \cdot (\alpha_a \mu_a \nabla \mathbf{v}_a) + K_{as}(\mathbf{v}_s - \mathbf{v}_a) + \alpha_a \rho_a \mathbf{g}$$

Momentum balance for liquid steel:

$$\frac{\partial(\alpha_s \rho_s \mathbf{v}_s)}{\partial t} + \nabla \cdot (\alpha_s \rho_s \mathbf{v}_s \mathbf{v}_s) = -\alpha_s \nabla p + \nabla \cdot (\alpha_s (\mu_s + \mu_t) \nabla \mathbf{v}_s) + K_{as}(\mathbf{v}_a - \mathbf{v}_s) + \alpha_s \rho_s \mathbf{g}$$

$$K_{as} = \frac{3}{4}\frac{C_D}{D_b}\alpha_s \rho_s |\mathbf{v}_s - \mathbf{v}_a|, \quad C_D = \frac{24}{\mathrm{Re}_b}\left(1 + 0.15\,\mathrm{Re}_b^{0.687}\right), \quad \mathrm{Re}_b = \frac{\rho_s |\mathbf{v}_s - \mathbf{v}_a| D_b}{\mu_s}$$

$$\mu_t = C_\mu \rho_s \frac{k^2}{\varepsilon}$$

Volume fraction equation: $$\alpha_s + \alpha_a = 1$$

Another Multiphase Flow Model – Discrete Phase Bubble Model

- **Lagrangian bubble tracking, calculate the bubble trajectories**

$$m_p \frac{d\mathbf{v}_p}{dt} = \underbrace{\mathbf{F}_D}_{\text{Drag force}} + \underbrace{\mathbf{F}_L}_{\text{Lift force}} + \underbrace{\mathbf{F}_{added-mass}}_{\text{Added mass force}} + \underbrace{\mathbf{F}_G}_{\text{Gravity}} + \underbrace{\mathbf{F}_{press} + \mathbf{F}_{stress}}_{\text{Pressure \& Stress gradient force}}$$

Motion: $\mathbf{v}_p = \dfrac{d\mathbf{x}_p}{dt}$

$$\mathbf{F}_D = \frac{1}{8}\pi d_p^2 \rho_f C_D \left|\mathbf{v}_f - \mathbf{v}_p\right| \left(\mathbf{v}_f - \mathbf{v}_p\right)$$

$$C_D = f_{\mathrm{Re}_p}\left(\frac{24}{\mathrm{Re}_p}\right), \mathrm{Re}_p = \left|\left(\mathbf{v}_f - \mathbf{v}_p\right)\frac{d_p}{\nu}\right|$$

$$f_{\mathrm{Re}_p} = \left(1 + 0.15\,\mathrm{Re}_p^{0.687}\right)$$

$$\mathbf{F}_G = \frac{\pi d_p^3}{6}\rho_p \mathbf{g}$$

$$\mathbf{F}_{press} + \mathbf{F}_{stress} = \frac{\rho_f \pi d_p^3}{6}\left(\frac{D\mathbf{v}_f}{Dt} - \mathbf{g}\right)$$

$$\mathbf{F}_{added-mass} = \frac{\rho_p \pi d_p^3}{12}\left(\frac{d\mathbf{v}_f}{dt} - \frac{d\mathbf{v}_p}{dt}\right)$$

$$\mathbf{F}_L = -\frac{9}{4\pi}\mu d_p^2 \mathbf{U}_s \,\mathrm{sgn}(G)\left[\frac{|G|}{\nu}\right]^{\frac{1}{2}} J^u$$

$$G = \mathbf{U}_s \times \left(\nabla \times \mathbf{v}_f\right), \quad \nabla\varepsilon = \mathrm{sgn}(G)\frac{\sqrt{|G|\nu}}{U_s}, \quad \mathbf{U}_s = \mathbf{v}_p - \mathbf{v}_f$$

$$J(\varepsilon) = 0.6765 * \left(1 + \tanh[2.5\lg\varepsilon + 0.191]\right)\left(0.667 + \tanh[6(\varepsilon - 0.32)]\right)$$

Ref:
(1) Maxey, M.R. and Riley, J.J.: Physics of Fluids, 1983, vol. 26 (4), pp. 883-889.
(2) Crowe, C., Sommerfild, M. and Tsinji, Y.: Multiphase Flows with Droplets and Particles, CRC Press, 1998, pp. 23-95.

Typical Argon-Steel Flow Pattern in SEN/Mold Region

- **Eulerian model simulation results:**

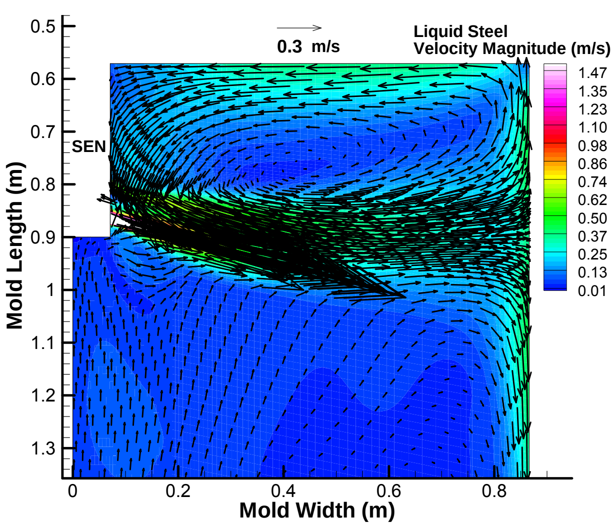

Mean bubble diameter: 2.56 mm (constant, based on nozzle flow model and initial bubble size estimation)

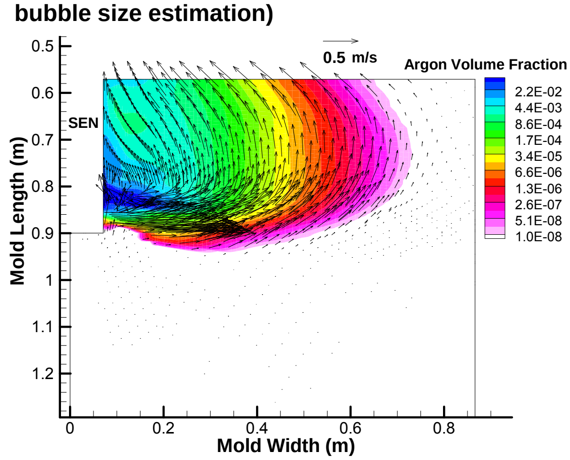

- **Double-roll flow pattern still exists with argon injection (~4% argon)**
- **Large scale instability (such as jet wobbling) has been reduced by gas injection comparing with single phase flow pattern in this case**

Comparison with Nail-Board Experiment Results – Board 4 Velocity Magnitude

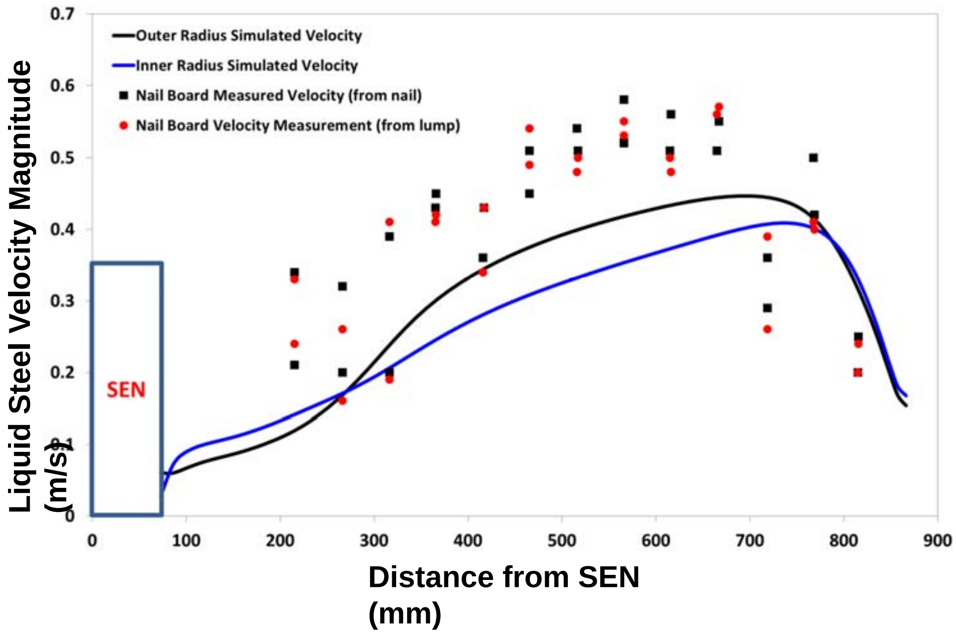

Comparison of Horizontal Velocity Profiles

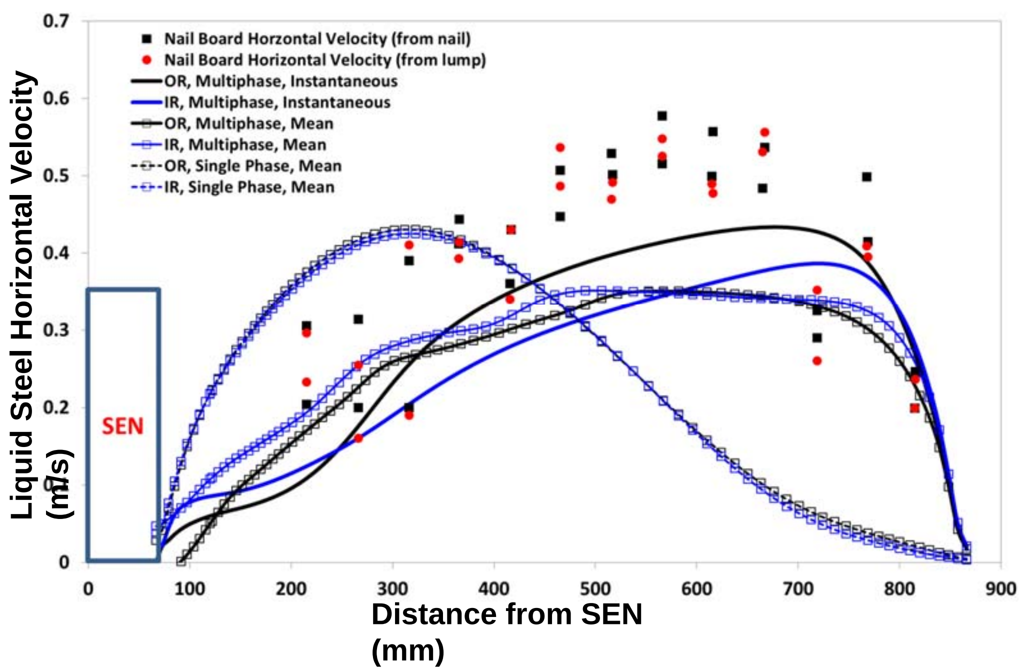

BOARD 4: DES with DPM

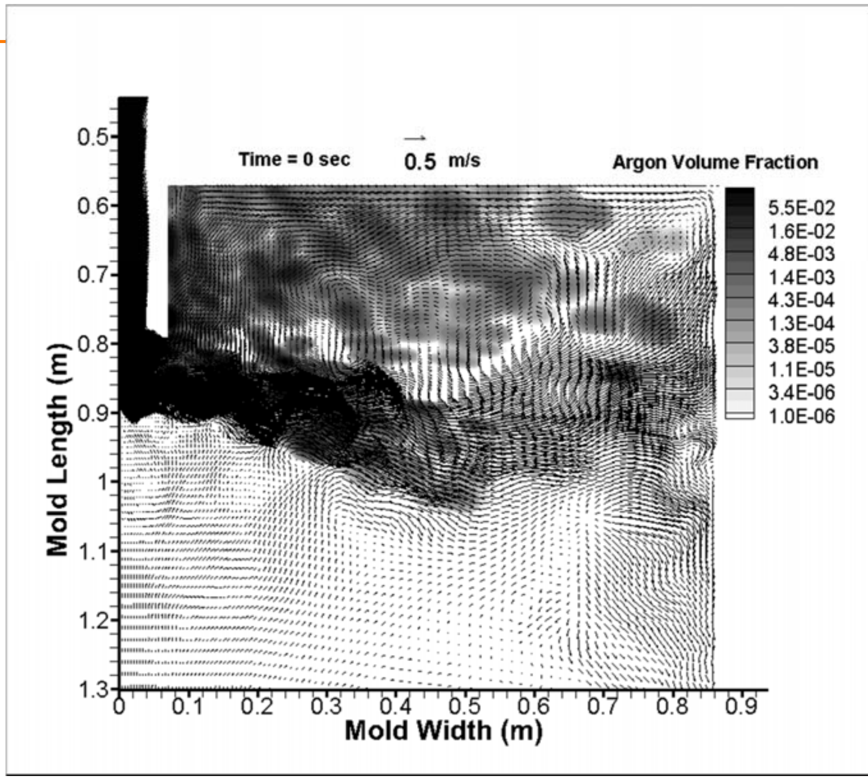

Comparison of Horizontal Velocity Profiles – Model vs. Measurements (Board 4)

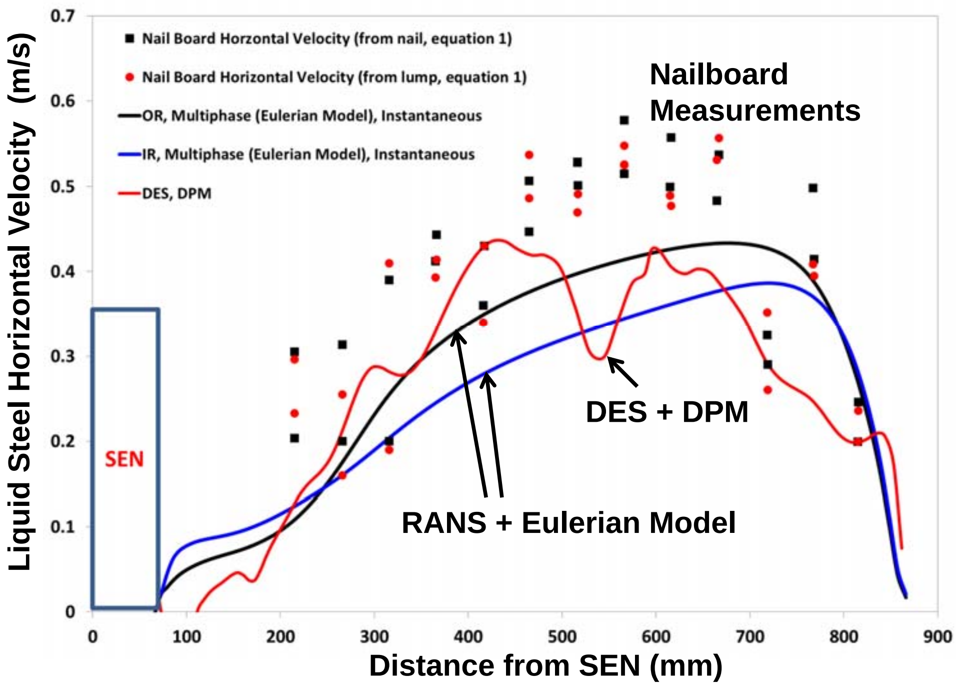

Comparison of Mold Level Profile (BOARD 4)

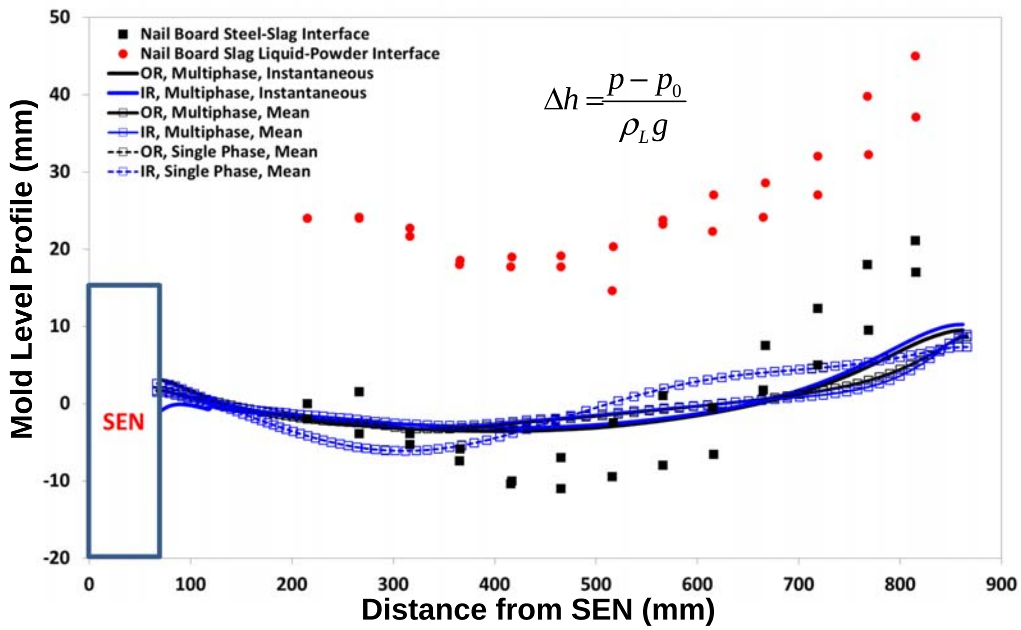

Conclusion – from BOARD 4 Simulation

- **Single phase flow simulation results show a wobbling liquid steel jet, which causes a periodical reverse flow away from SEN at regions close to the narrow face;**
- **Jet wobbling is reduced by adding a small amount of gas into the liquid steel (~4% in current case, board 4), and the double-roll flow pattern still remains;**
- **Comparison of liquid steel surface velocity with nail board measurements suggests:**
  - **the trend of both instantaneous and mean steel surface velocity distributions from argon-steel two-phase simulations match well with nail-board measurements (with velocities peak closer to narrow face), but with a ~20-30% velocity magnitude difference;**
  - **single phase simulation results suggest an opposite velocity distribution – velocity peaks close to SEN instead of narrow face;**

Conclusion – from BOARD 4 Simulation (CONT.)

- DPM model is promising in multiphase flow modeling, given:
  - A high resolution mesh
  - More accurate turbulence model (LES e.g.)
  - A well-educated bubble size distribution

Simulations for BOARD 11~13

Date & Time	Nailboard Case #	Casting Speed (inch/min)	Strand Width (inch)	Argon Flow Rate (SLPM)	Argon Back Pressure (psi)	Submerging Depth (mm)
10/16, 3:28:54 pm	11	65.0	54.99	7.0	18.07	222
10/16, 3:29:20 pm	12	65.0	54.99	7.0	18.07	222
10/16, 3:29:41 pm	13	65.0	54.99	7.0	18.07	222

- In this part of work, the following techniques and parameters are utilized:
  - RANS model (k-epsilon) for turbulence
  - Eulerian model for dispersed bubble phase
  - Two mean bubble diameters, 3mm and 5mm, are studied
  - Mold top surface profile is calculated using:
    - Pressure method
    - A moving-grid free surface tracking algorithm

Liquid Steel Velocity Distribution at Mold Center Plane

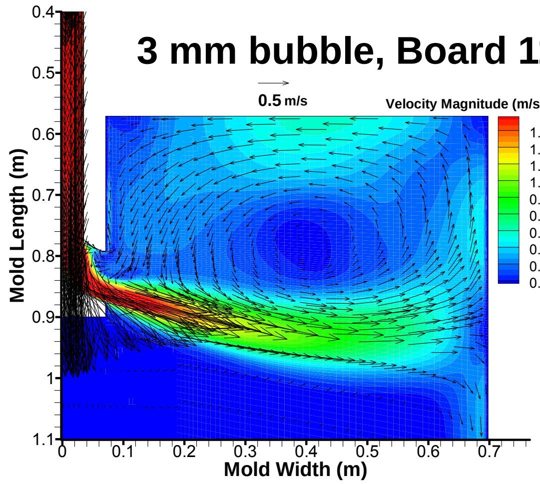

3 mm bubble, Board 11~13

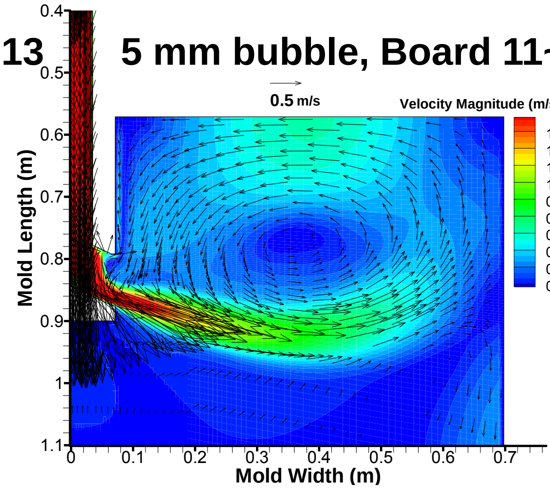

5 mm bubble, Board 11~13

- **Double-roll flow pattern achieved for both 3 mm bubble and 5 mm bubble**
- **Slightly higher sub-meniscus velocity is found for 5 mm bubble size case**

Argon Gas Velocity / Fraction Distribution at Mold Center Plane

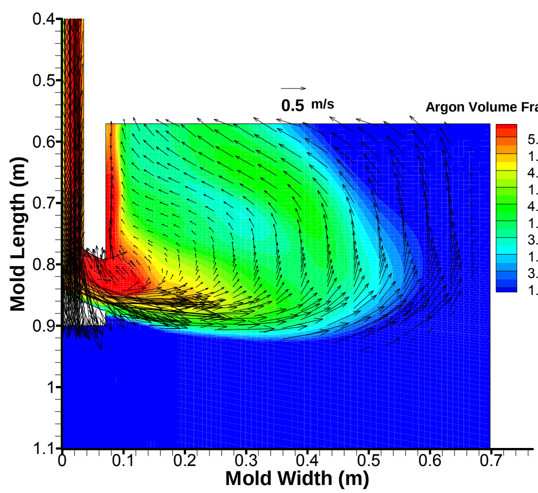

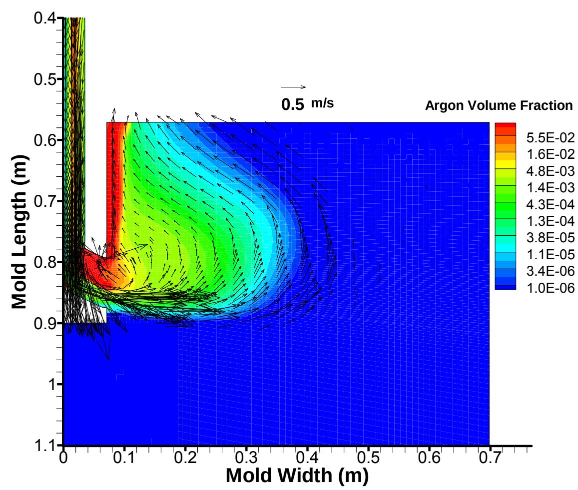

3 mm bubble, Board 11~13 5 mm bubble, Board 11~13

- **Gas with 3 mm bubble size spreads further into the liquid pool, closer to the narrow phase, comparing with the case with 5 mm bubble size**

Liquid Steel Velocity Distribution at Mold Top Surface

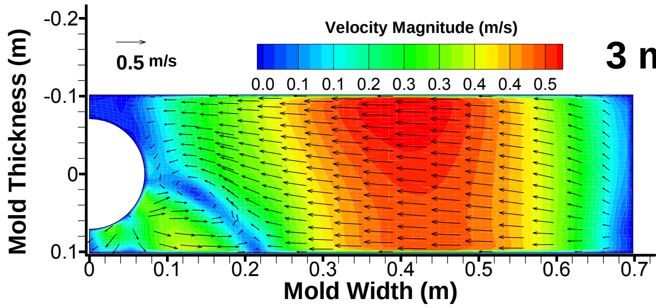

3 mm bubble, Board 11~13

- Higher surface velocity found in 5 mm bubble size case

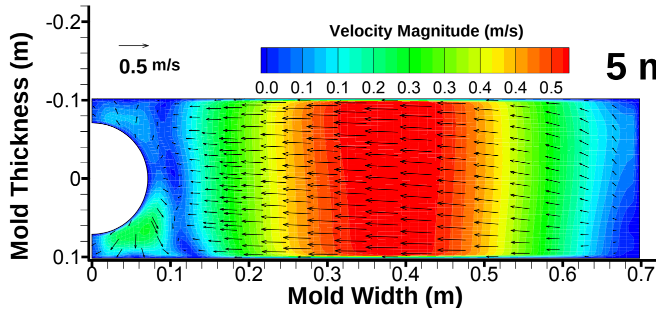

5 mm bubble, Board 11~13

Argon Gas Velocity / Fraction Distribution at Mold Top Surface

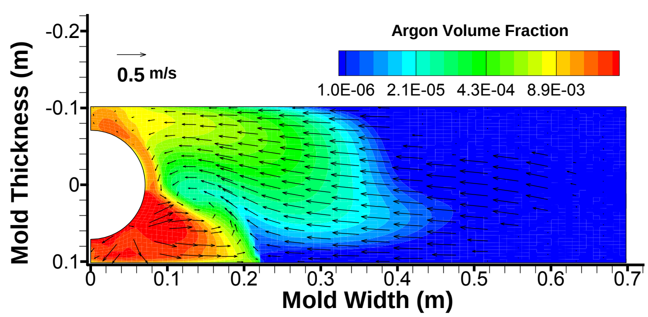

3 mm bubble, Board 11~13

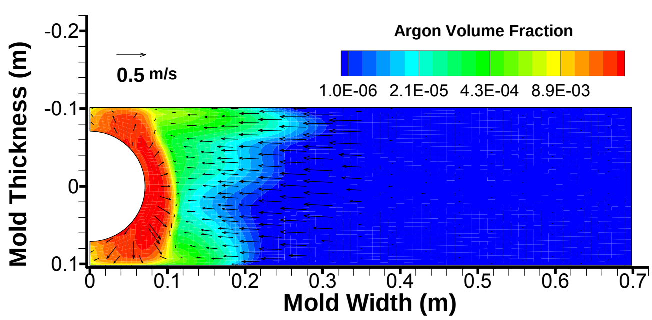

5 mm bubble, Board 11~13

Argon Gas Velocity / Fraction Distribution at Port Exit

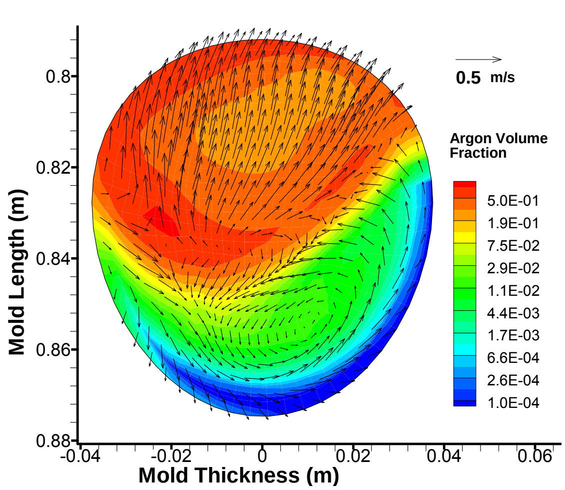

3 mm bubble, Board 11~13

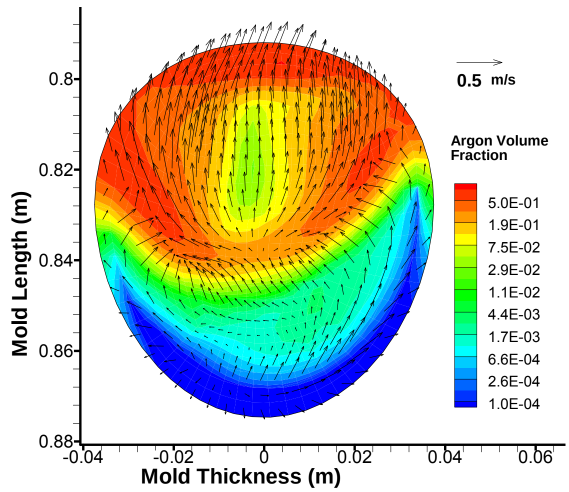

5 mm bubble, Board 11~13

- **Higher gas rising velocity found in 5 mm bubble size case at port exit**

Liquid Steel Velocity Distribution at Port Exit

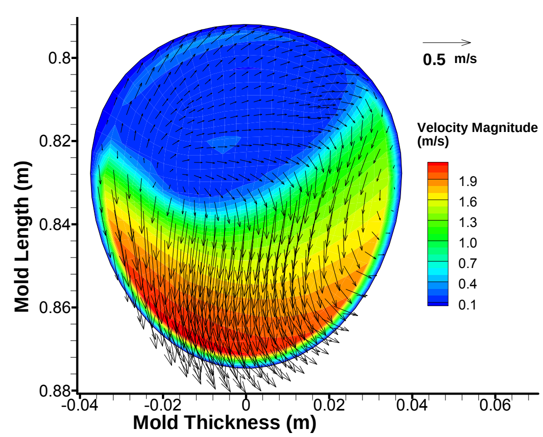

3 mm bubble, Board 11~13

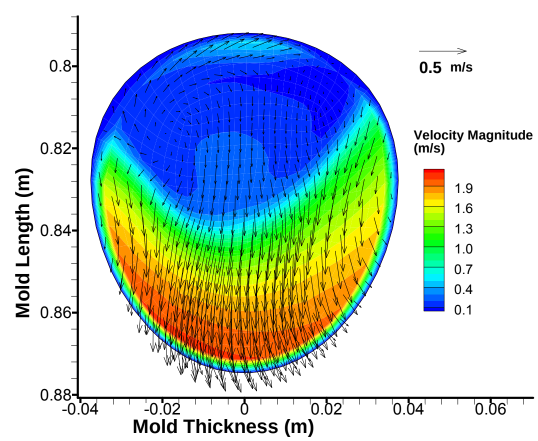

5 mm bubble, Board 11~13

Free Surface Modeling

- **Pressure Conversion**
  - **Wall boundary condition at domain top surface**
  - **Best used for steady / quasi-steady state flows, without gravity waves**
    - **Lifting**
    - **displacement**
- **Moving-grid Surface Tracking ***
  - **Pressure boundary at domain top surface**
  - **Working for both steady state and transient flows, with/without gravity waves**

* R. Liu, B.G. Thomas, L. Kalra, T. Bhattacharya, and A. Dasgupta., *Proc. AISTech 2013 Conf.* (Pittsburg, PA), p1351-1364, (2013)

Moving Grid Technique using FVM

Continuity equation with moving mesh:

$$\nabla \cdot \left(\rho \left(\mathbf{v} - \mathbf{v}_g \right) \right) = 0$$

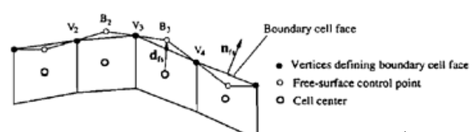

$$\dot{m}_{fs} + \rho \dot{V}'_{fs} = 0$$

Momentum equation with moving mesh:

$$\frac{\partial (\rho \mathbf{v})}{\partial t} + \nabla \cdot \left(\rho \mathbf{v} \left(\mathbf{v} - \mathbf{v}_g \right) \right) = -\nabla p + \nabla \cdot (\mu \nabla \mathbf{v}) + \mathbf{F}$$

V is fluid velocity, while V_g is grid velocity (mesh velocity)

$$\Delta h = \gamma_{fs} \frac{\dot{V}'_{fs} \Delta t}{S_{fs} \mathbf{n} \cdot \mathbf{e}_{fs}}$$

$$\mathbf{r}_{B_i}^{k+1} = \mathbf{r}_{B_i}^{k} + \Delta h \, \mathbf{e}_{fs}$$

$$\mathbf{r}_{V_i}^{k+1} = \mathbf{r}_{V_i}^{k} - \mathbf{e}_{fs} \cdot \left[\mathbf{r}_{V_i}^{k} - \sum_{m=1}^{n} w_m \mathbf{r}_{B_m}^{k+1} \right] \mathbf{e}_{fs}$$

Kinematic B.C.:

$$\left[\left(\mathbf{v} - \mathbf{v}_s \right) \cdot \mathbf{n} \right]_{fs} = 0 \quad \text{or} \quad \dot{m}_{fs} = 0$$

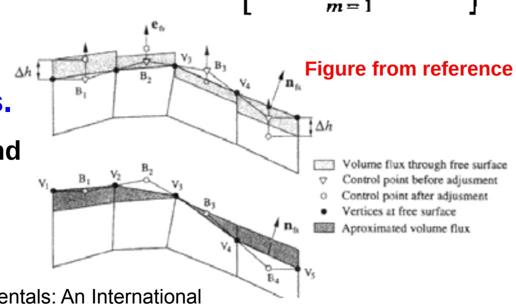

Figure from reference

Dynamic B.C.: all forces in equilibrium at fs.

This node moving approach has been adopted and coded into FLUENT udf for free surface modeling in current work

Ref:

S. Muzaferija and M. Peri´c, Numerical Heat Transfer, Part B: Fundamentals: An International Journal of Computation and Methodology, 1997. Vol 32:4, 369-384

Large Amplitude Sloshing

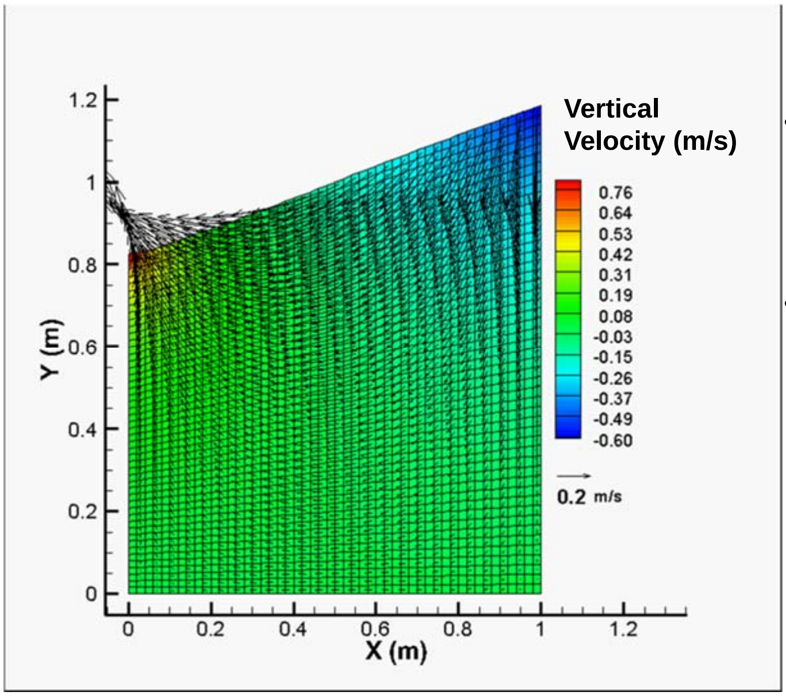

- **Free surface nodes moved via UDF, with kinematic and dynamic B.C.s satisfied**
- **Side wall nodes and internal nodes are smoothed via solution of a Laplace equation diffusing free surface nodes displacements to interior nodes**

Model Validation – Analytical Solution and Case Setup

- **2-D small-amplitude sloshing problem**

$$a(t)=\frac{4\nu^2k^4}{8\nu^2k^4+\omega_0^2}a_0\,erfc\left(\nu k^2 t\right)^{\frac{1}{2}}+\sum_{i=1}^{4}\frac{z_i}{Z_i}\left(\frac{\omega_0^2 a_0}{z_i^2-\nu k^2}\right)\exp\left(\left(z_i^2-\nu k^2\right)t\right)erfc\left(z_i t^{\frac{1}{2}}\right)$$

Where z_i is the i^{th} root of the equation below, and z_i is defined as:

$$z^4+2\nu k^2 z^2+4\left(\nu k^2\right)^{\frac{3}{2}}z+\nu^2k^4+\omega_0^2=0 \qquad \omega_0=\sqrt{gk}$$

Prosperetti, A., 1981. “Motion of two superposed viscous fluids”. Physics of Fluids, 24(7), July, pp. 1217–1223.

Initial Interface: $h(x)=1.5+a_0\sin\left(\pi(0.5-x)\right)$

a_0=0.01 m

Level Height (mm)	Tank Width (mm)	Initial Perturbation Amplitude (mm)
1500	1000	20

Fluid Kinematic Viscosity (m^2/s)	Gravity Acceleration (m/s^2)	Surface Tension (N/m)
0.01	1.0	0

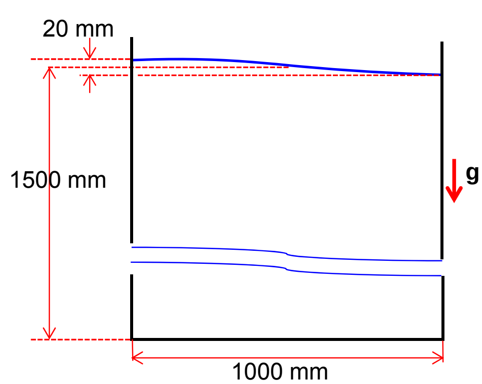

Model Validation – Comparison with Analytical Solution

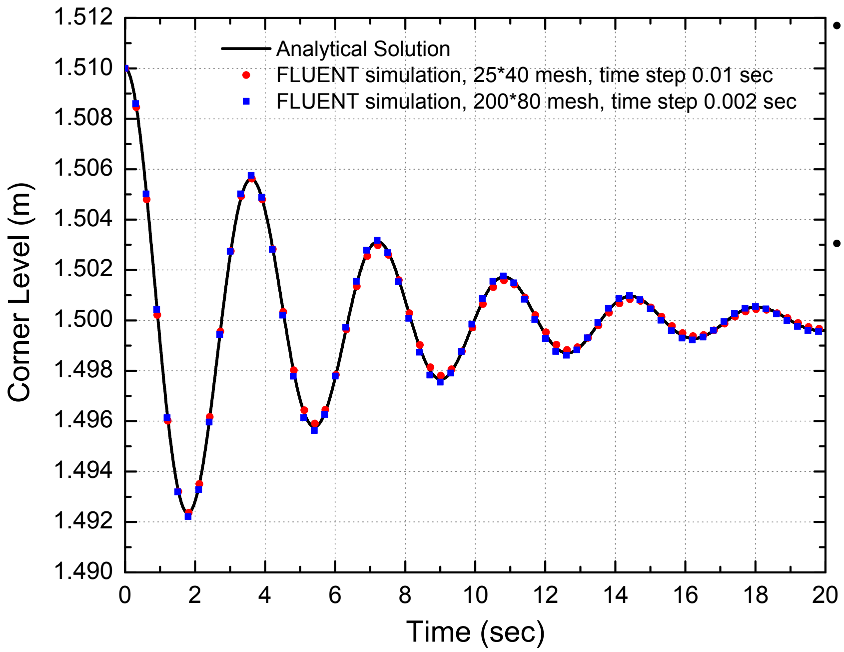

- **Excellent match with analytical solution obtained even for simulations using the very coarse mesh**
- **Using second order (or higher) advection scheme and temporal scheme are crucial for achieving accuracy**

Liquid Steel Velocity Distribution at Mold Center Plane (Board 11-13)

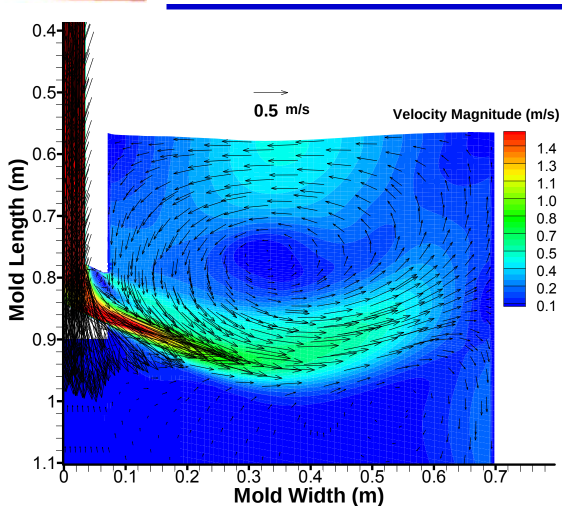

Single Phase, Board 11~13

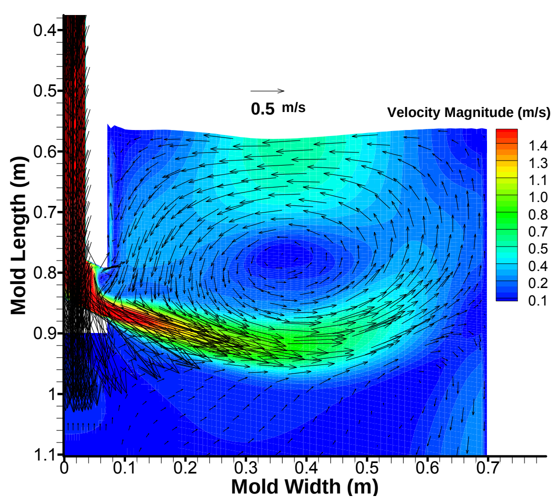

Multiphase, Board 11~13 (5 mm bubble size)

- **Gas injection (with 5 mm bubble size) increases liquid steel surface velocity, and surface level difference**

Moving-Grid Free Surface Tracking Single Phase vs. Two-Phase Flow

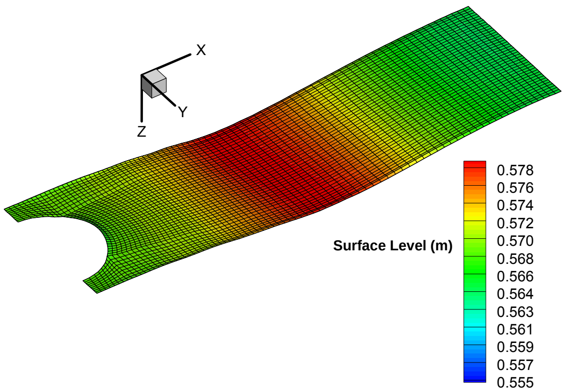

Single Phase, Board 11~13

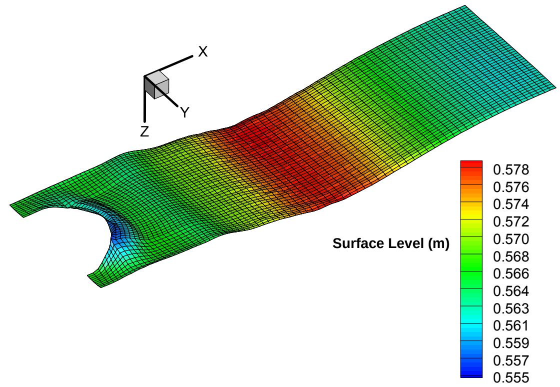

Multiphase, Board 11~13 (5 mm bubble size)

- **Rising of gas bubbles elevate the surface level near SEN, comparing with the no-gas case**

Liquid Steel Velocity Distribution – Wall B.C. vs. Pressure B.C.

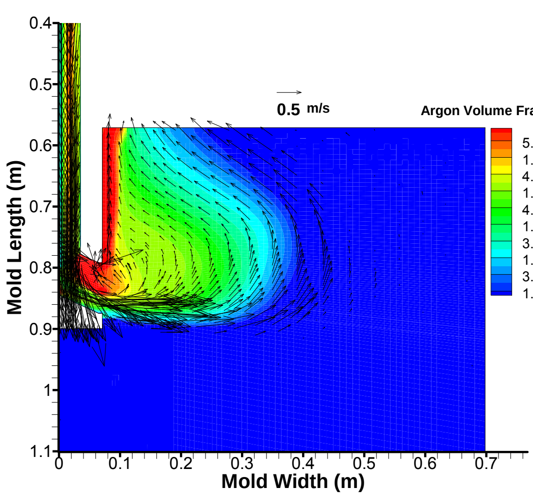

5 mm bubble, Board 11~13 (wall B.C. on top)

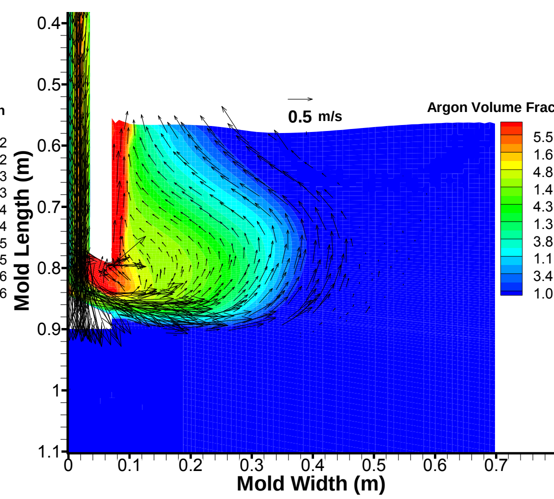

5 mm bubble, Board 11~13 (free surface tracking, pressure B.C. on top)

- **No significant change for the gas distribution using either method**

Comparison with Nail Board Measurements – Horizontal Velocity

(Board 11-13)

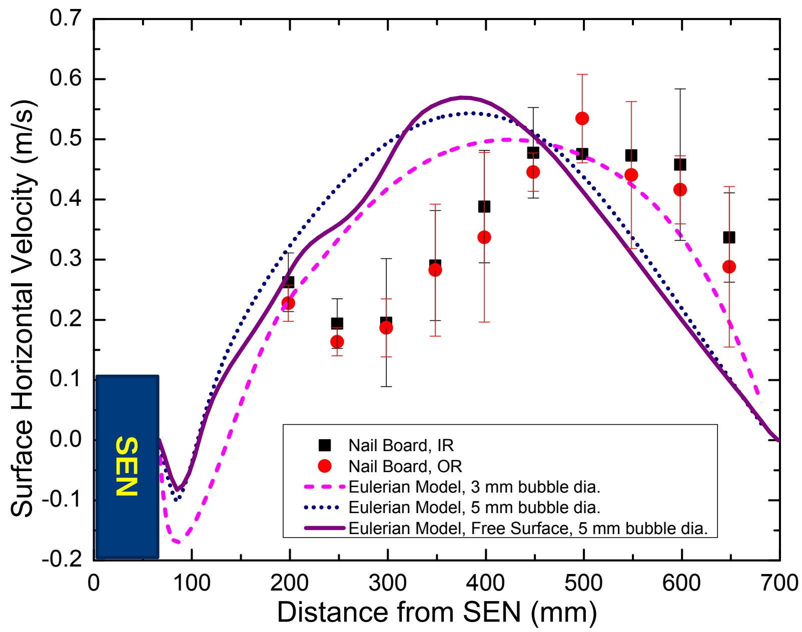

Comparison with Nail Board Measurements – Surface Level Profile

(Board 11-13)

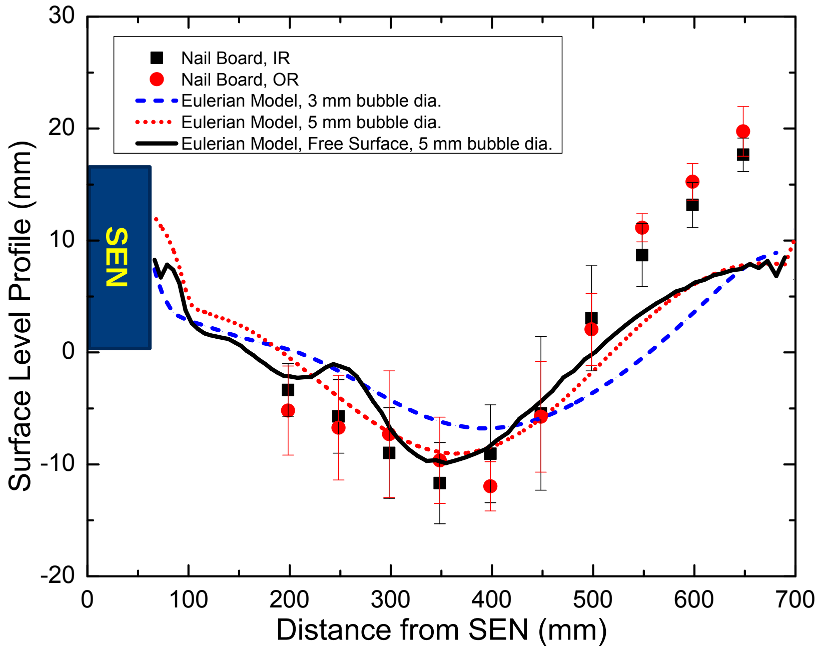

Conclusions – from BOARD 11~13

- Single phase flow simulation results does not show any wobbling liquid steel jet, thus narrower mold generates a more stable flow pattern comparing to the wider mold (shown previously in case 4)
- Smaller bubble size (3 mm) increases surface velocity slightly, while larger bubbles (5 mm)
  - increase the surface velocities significantly and
  - increase surface level differences
- Simple pressure method and moving-grid method predict similar surface level profiles
- The 5-mm bubble case matches reasonably with measurements (better than with 3mm dia.)
- Better match near NF could be obtained if the nailboard had been tilted

Simulations for BOARD 14~16

Date & Time	Nailboard Case #	Casting Speed (inch/min)	Strand Width (inch)	Argon Flow Rate (SLPM)	Argon Back Pressure (psi)	Submergence Depth (mm)
10/16, 3:35:50 pm	14	25.5	54.99	6.3	19.18	222
10/16, 3:36:16 pm	15	25.5	54.99	6.2	19.18	222
10/16, 3:36:36 pm	16	25.5	54.99	6.2	19.18	222

- In this part of work, the following techniques and parameters are utilized:
  - RANS model (k-epsilon) for turbulence
  - Eulerian model for dispersed bubble phase
  - Three mean bubble diameters, 3mm, 5mm and 8mm, are studied

Liquid Steel Velocity Distribution at Mold Center Plane – Board 14~16

5 mm bubble, Board 14~16

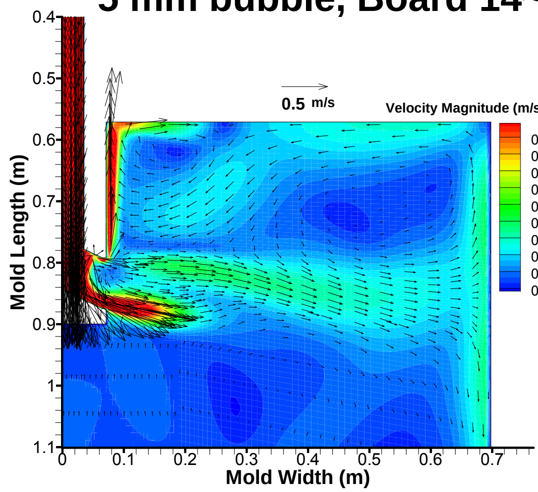

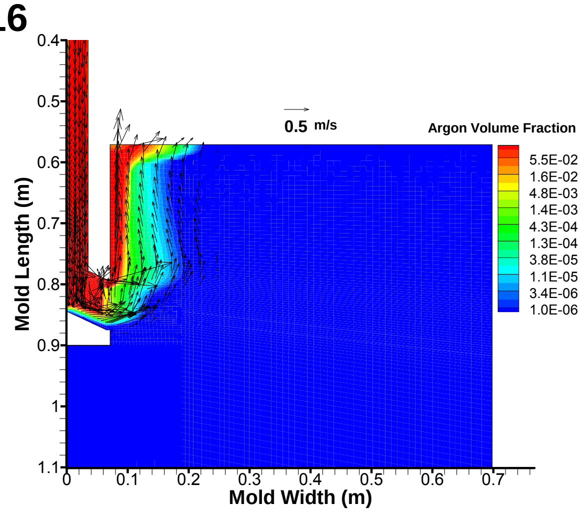

Complex flow pattern with partial reversed flow

Rising argon bubbles concentrate near SEN

Velocity / Argon Fraction Distribution at Mold Top Surface – Board 14~16

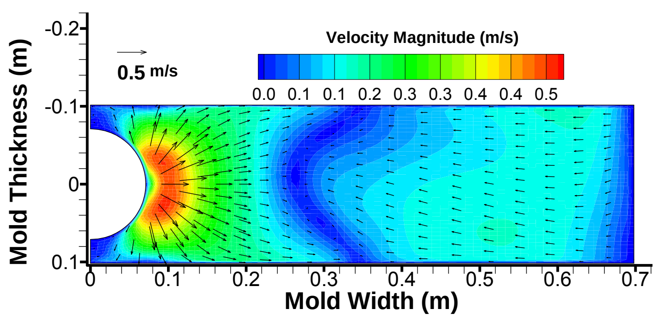

- **Two liquid steel surface streams move in opposite directions, and meet in the middle region**

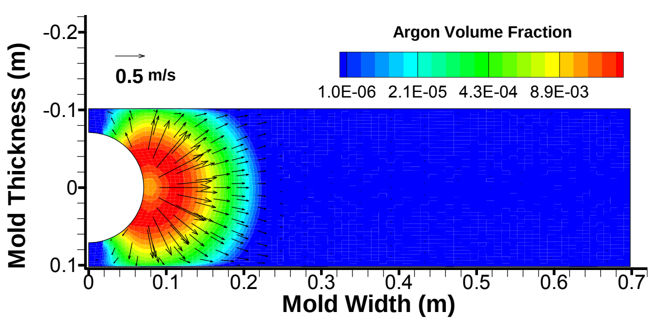

- **Gas exits to the top surface in a symmetric manner, indicating less affected by the swirling liquid steel jet**

Liquid Steel Velocity / Gas Distribution at Port Exit

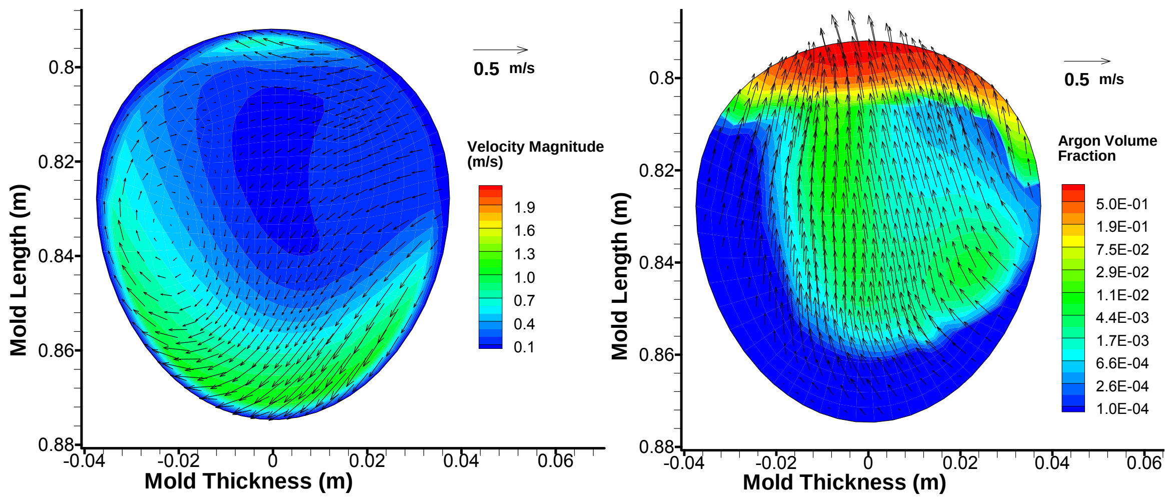

Comparison with Nail Board 14~16 Measurements – Horizontal Velocity

(Board 14-16)

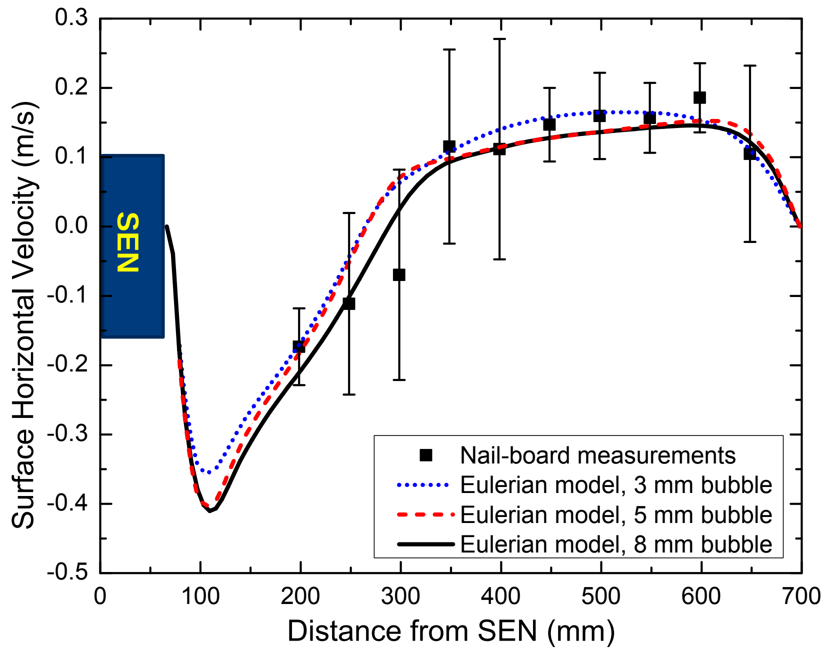

Comparison with Nail Board 14~16 Measurements – Mold Level

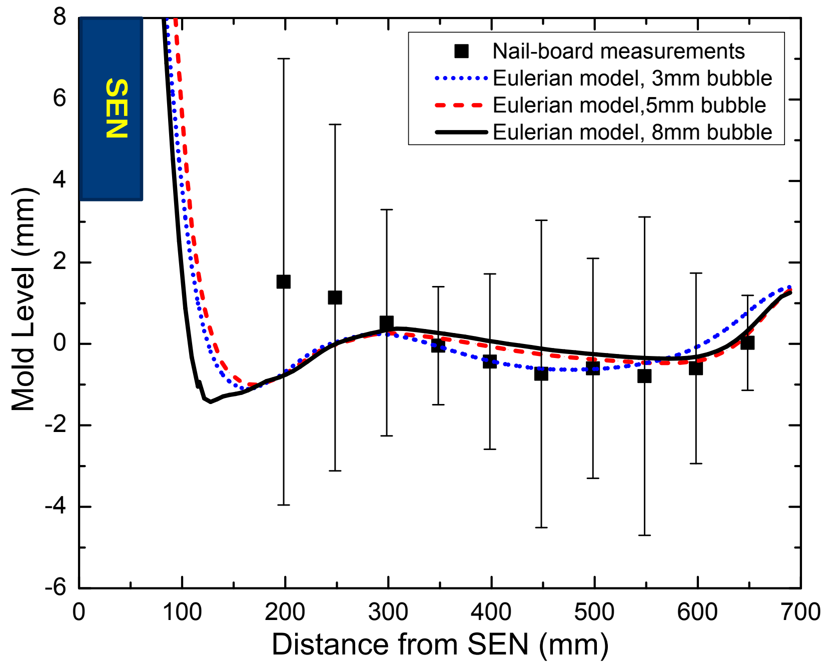

(Board 14-16)

Conclusion – from BOARD 14~16

- **Excellent match is found between the measured and predicted surface steel velocities, as well as for the mold level, for all three bubble diameters used (3, 5 and 8 mm);**
- **Detailed comparison between simulations and measurements indicates that utilization of multi-size bubble groups instead of a single mean bubble size would increase the accuracy.**

Summary and Future Work

- Methodology of modeling and simulating argon-steel multi-phase nozzle/mold flows has been established
- Models have been validated with many measurements and reasonable accuracy has been achieved for flow patterns, including complex flows with partial surface reversals due to gas bubbles rising
- Future work includes:
  - Develop and apply criteria for defects formation
  - Parametric studies to classify flows
  - Use methodology and models in this work to find operation windows to avoid defects